Ocean Sci. Discuss., 9, 2621–2677, 2012
www.ocean-sci-discuss.net/9/2621/2012/
doi:10.5194/osd-9-2621-2012

Ocean Science Discussions

Time and space variability of freshwater content, heat content and seasonal ice melt in the Arctic Ocean from 1991 to 2011

M. Korhonen[1,2], B. Rudels[1,2], M. Marnela[1,2], A. Wisotzki[3], and J. Zhao[4]

[1]Finnish Meteorological Institute, Helsinki, Finland
[2]Department of Physics, University of Helsinki, Helsinki, Finland
[3]Alfred Wegener Institute, Bremerhaven, Germany
[4]College of Physical and Environmental Oceanography, Ocean University of China, Qingdao, China

Received: 6 June 2012 – Accepted: 26 June 2012 – Published: 1 August 2012

Correspondence to: M. Korhonen (meri.korhonen@fmi.fi)

Published by Copernicus Publications on behalf of the European Geosciences Union.

Abstract

The Arctic Ocean gains freshwater mainly through river discharge, precipitation and the inflowing low salinity waters from the Pacific Ocean. In addition the recent reduction in sea ice volume is likely to influence the surface salinity and thus contribute to the freshwater content in the upper ocean. The present day freshwater storage in the Arctic Ocean appears to be sufficient to maintain the upper ocean stratification and to protect the sea ice from the deep ocean heat content. The recent freshening has not, despite the established strong stratification, been able to restrain the accelerating ice loss and other possible heat sources besides the Atlantic Water, such as the waters advecting from the Pacific Ocean and the solar insolation warming the Polar Mixed Layer, are investigated. Since the ongoing freshening, oceanic heat sources and the sea ice melt are closely related, this study, based on hydrographic observations, attempts to examine the ongoing variability in time and space in relation to these three properties.

The largest time and space variability of freshwater content occurs in the Polar Mixed Layer and the upper halocline. The freshening of the upper ocean during the 2000s is ubiquitous in the Arctic Ocean although the most substantial increase occurs in the Canada Basin where the freshwater is accumulating in the thickening upper halocline. Whereas the salinity of the upper halocline is nearly constant, the freshwater content in the Polar Mixed Layer is increasing due to decreasing salinity. The decrease in salinity is likely to result from the recent changes in ice formation and melting. In contrast, in the Eurasian Basin where the seasonal ice melt has remained rather modest, the freshening of both the Polar Mixed Layer and the upper halocline is mainly of advective origin.

While the warming of the Atlantic inflow was widespread in the Arctic Ocean during the 1990s, the warm and saline inflow events in the early 2000s appear to circulate mainly in the Nansen Basin. Nevertheless, even in the Nansen Basin the seasonal ice melt appears independent of the continuously increasing heat content in the Atlantic layer. As no other oceanic heat sources can be identified in the upper layers, it is likely

that increased absorption of solar energy has been causing the ice melt prior to the observations.

1 Introduction

Direct precipitation and runoff provide two thirds of the total freshwater input to the Arctic Ocean whereas approximately one third derives from the low salinity Pacific water imported through the Bering Strait (Aagaard and Carmack, 1989; Dickson et al., 2007). Due to the fairly open pathways between the Arctic and Atlantic oceans most of the oceanic heat is transported to the Arctic Ocean through Fram Strait and Barents Sea. Particularly the heat content carried by the Fram Strait branch is nearly conserved as the warm and saline Atlantic Water becomes decoupled from the atmosphere north of Svalbard, where a relatively fresh surface layer is formed by mixing with ice melt. The passage between the Arctic and Pacific oceans is more restricted and the volume transport through the Bering Strait is only one tenth of that from the Atlantic. Nevertheless, the Pacific waters are, at least during summer, relatively warm and fresh (Stigebrandt, 1984) and, due to their low density, import heat closer to the ocean surface and sea ice compared to the Atlantic Water.

Generally the large freshwater input and storage are considered as a precondition for the maintenance of the perennial ice cover in the Arctic Ocean. The freshwater flux stabilises the surface layer and insulates sea ice from heat stored in the Atlantic layer (Aagaard et al., 1981; Rudels et al., 1996). Typically not even the convection induced by ice formation and associated brine rejection is able to reach the thermocline. Only in the Southern Nansen Basin the weaker stratification, due to the relatively high surface salinity, enables deeper winter convection and possible upward mixing of the warm Atlantic Water. However, changes in wind driven ocean advection have previously been observed to disturb the stratification even beyond the Nansen Basin (Proshutinsky and Johnson, 1997; Steele and Boyd, 1998).

In the late 1980s and early 1990s the prevailing atmospheric circulation pattern, described by the Arctic Oscillation (AO) index (Thompson and Wallace, 1998), was considered to largely regulate changes in the Arctic freshwater content, heat content and seasonal ice melt. The amplified ice export through the Fram Strait together with the enhanced Atlantic heat flux to the sea ice were suggested to be the key contributors to the accelerated decline in sea ice extent (Maslanik et al., 1996; Vinje, 2001; Rigor et al., 2002). The export of freshwater (Karcher et al., 2005) and sea ice had further consequences in the Nordic Seas where the formation of the North Atlantic Deep Water was reduced (Dickson, 1996).

Despite the change in wind driven circulation in the late 1990s, now favouring the accumulation of freshwater and consequent strengthening of the stratification in large parts of the Arctic Ocean (Björk et al., 2002; Boyd et al., 2002; Proshutinsky et al., 2009), the sea ice volume has continued to diminish with startling speed (Lindsay and Zhang, 2005; Stroeve et al., 2007). Thus, although the formation of the halocline is still regarded essential for providing insulation between the Atlantic heat and the sea ice, the heat stored in the Atlantic layer is no longer considered as the main threat to the perennial ice cover. Whereas the freshwater flux has protected the ice cover from oceanic heat fluxes, the high albedo of sea ice has limited the amount of solar radiation penetrating the ice-ocean system. During the past two decades declining ice cover, leading to reduced surface albedo, has crucially altered the heat budget of the Polar Mixed Layer (Maykut and McPhee, 1995; Perovich et al., 2007a).

Since the heat entering the Polar Mixed Layer eventually either is consumed by ice melt or lost to the atmosphere, the surface temperature generally remains near the freezing point and the heat content in the Polar Mixed Layer is practically negligible (Coachman and Barnes, 1961). However, a seasonal temperature maximum around depth 20–30 m, not yet observed by Coachman and Barnes, was seen during AIDJEX (Arctic Ice Dynamics Joint Experiment) in 1975. Maykut and McPhee (1995) attributed this feature to increased short wave radiation. Since then the near surface temperature maximum has become more pronounced, indicating that the amount of absorbed solar

OSD
9, 2621–2677, 2012

radiation has increased, particularly in the Chukchi and Southwestern Beaufort seas where the most notable ice loss has occurred during the past decades (McPhee et al., 1998; Shimada et al., 2001; Perovich et al., 2008; Jackson et al., 2010).

In addition to the role of radiative processes in recent ice loss, the Bering Strait waters have been suggested to supply additional heat to the upper ocean. Previously the modest heat content in the waters deriving from the Pacific Ocean was presumed to be negligible but the direct measurements of the Bering Strait transports since the early 1990s revealed high variability in both volume and temperature of the Bering Strait inflow (Roach et al., 1995; Woodgate et al., 2010). Although no permanent increasing trend in temperature or heat content is yet documented, Shimada et al. (2001) and Steele et al. (2004) proposed a possible warming of the Alaskan Coastal Water during the late 1990s, and more recently Woodgate et al. (2010) discussed the anomalously large heat imports to the Arctic Ocean through the Bering Strait in 2004 and 2007, the latter being due to both increased volume and temperature. Furthermore Shimada et al. (2006) noted that the atmospheric forcing could influence the spreading of the relatively warm Alaskan Coastal Water northward and thus accelerate the ice loss.

The freshwater content, heat content and seasonal ice melt have been widely studied, but only seldom have they been discussed together. By dividing the upper 1000 dbar of the water column into six water masses and distinguishing the meltwater from the freshwater in the Polar Mixed Layer, the present study aims to reveal connections between the changing characteristics of each water mass. Oceanographic observations are used to examine possible heat sources in the upper ocean and to assess the role of sea ice loss in the recent freshening of the Arctic Ocean. Also the horizontal variability is taken into account in discussing the changes occurring in the Arctic hydrography during the past two decades. Even the sparse data sets used in this study are found to agree surprisingly well with other corresponding studies and thus the comprehensive approach used here is assumed reliable in assessing recent changes in the Arctic Ocean.

OSD
9, 2621–2677, 2012

2 Approach

2.1 Data

The analysed hydrographic data are obtained from selected icebreaker cruises conducted in July–September. They cover the 20 yr period from 1991 to 2011 and offer summertime snapshots on the local conditions. Data are collected as conductivity-temperature-depth (CTD) surveys, from which potential temperature and salinity profiles are analysed to distinguish the different water masses and further compute freshwater content, heat content and seasonal ice melt as described below in this chapter. Figure 1 and Table 1 offer more information on the cruises. Table 1 also includes references for more specific information on the used instruments and their accuracies.

Like the passages regulate the water exchange between the Arctic Ocean and the world ocean, so also the bathymetry of the Arctic Ocean influences the spreading of waters originating from the Atlantic and Pacific oceans and thus determines the characteristics of each sub-basin. To review the horizontal distribution of water masses and variability of freshwater and heat contents, the bathymetry is used to divide the Central Arctic Ocean into eight sub-areas (Fig. 2). The Lomonosov Ridge extends from north of Greenland across the North Pole to the Siberian shelf and thus divides the Arctic Ocean into the Eurasian and Amerasian basins. The Eurasian Basin includes the Nansen and Amundsen basins, separated by the Gakkel Ridge. The Amerasian Basin is divided into the Canada Basin and the Makarov Basin by the Alpha and Mendeleyev ridges. Although the Alpha and Mendeleyev ridges are separated by a 2500 m deep gap, they are in this study discussed together. The Canada Basin is divided into a southern and a northern part by latitude 78° N and the Chukchi Plateau.

2.2 Representativeness of data

The unfortunate fact remains that icebreaker cruises are limited in their spatial extent, sometimes covering rather a basin-wide section than an extensive area. As seen in

OSD
9, 2621–2677, 2012

Fig. 1, the insufficient horizontal coverage represents uncertainties in the data analysis. Also the large time gaps add difficulties to the interpretation. Particularly in the Canada Basin the data from 1990s are more limited in time and space compared to the data sets from 2000s.

This raises a question about the spatial representativeness of data and its interannual comparability. The coarseness of available data is illustrated by the coverage percentages approximated from the grid shown in Fig. 1 and presented in Table 1. The coverage in a grid sell is set to 100 % when any number of casts are available within the cell. The most extensive data coverage is attained in the Nansen and Amundsen basins, however, also there the coverage reaches at highest only 50 %.

2.3 Water masses

In the intermediate and deep layers, the time and space variability of salinity and temperature is modest and slow compared to the uppermost 1000 dbar. Therefore the freshwater and heat contents are studied only in the upper 1000 dbar, which is here separated into six water masses with distinct properties (Fig. 3, Table 2). It should be noted, however, that apart from the definitions adopted here several other classifications and names of the water masses, especially of the halocline waters, exist (e.g. Guay and Falkner, 1997; Kikuchi et al., 2004; Steele et al., 2004; Proshutinsky et al., 2009).

Following Rudels et al. (1996) the thickness of the Polar Mixed Layer (PML) is defined by the temperature minimum, considered as a remnant of the previous winter convection. If the temperature minimum is absent or ambiguous, the rapid change in the magnitude of the salinity gradient may be of assistance: the steepening of the salinity gradient often begins immediately below the temperature minimum. The upper halocline (UHC) is here defined as the layer between temperature minimum and salinity 34. The upper halocline derives mainly from the Bering Strait inflow and consists of three different water masses: Alaskan Coastal Water (ACW), Bering Sea Summer Water (BSSW) and Bering Sea Winter Water (BSWW). In addition the runoff from the

Siberian rivers leads to low salinity shelf water in the upper halocline salinity range. The absence of both the Pacific derived waters and the river runoff generally leads to a weak or absent upper halocline in the Central Nansen Basin where the average salinity of the Polar Mixed Layer is typically higher than 34.

A lower halocline (LHC) is generally formed when the saline surface layer in the Nansen Basin advects further into the Arctic Ocean and becomes submerged by low salinity shelf water that enters the deep basins mainly from the Laptev Sea and other marginal seas farther east (Rudels et al., 1996). Because of its origins, the upper boundary of the lower halocline is set to isohaline 34. The Arctic Atlantic Water is commonly defined with temperatures above zero and thus the zero-isotherm marks the boundary between the lower halocline and Atlantic layer. As a consequence the lower halocline also comprises the upper part of the thermocline. The temperature maximum is used to separate the Atlantic layer into an upper (AW1) and a lower (AW2) part. AW1 forms a generally warmer, fresher and thinner layer than the AW2.

The zero-isotherm also indicates the lower limit of the Atlantic Water. In the Eurasian Basin this lower limit for AW2 coincides closely with the depth of a salinity minimum, which originates from the modified Barents Sea branch of Atlantic Water (Rudels et al., 1994; Schauer et al., 1997). This inflow becomes less saline in the Barents Sea, but because of heat loss, its density increases and the densest water sinks below the Atlantic Water as it enters the Nansen Basin. Hence Rudels et al. defined this water mass as upper Polar Deep Water (UPDW) with potential temperature $-0.5^{\circ}\mathrm{C} < \theta < 0^{\circ}\mathrm{C}$, decreasing with depth, and with salinity $34.88 < S < 34.92$. In the Amerasian Basin salinity increases uniformly with depth and the salinity minimum disappears. Here the UPDW is identified simply by temperatures below zero. Note that the UPDW is cut off at $p = 1000\,\mathrm{dbar}$, although it reaches depth of roughly 1200 dbar.

Although the water masses, aside from the Polar Mixed Layer, are defined with unambiguous isotherms and isohalines, a caveat is represented by the internal waves which may shift the isopleths up or down. However, this error is assumed to disappear when averaging over large domains.

OSD
9, 2621–2677, 2012

2.4 Approach to freshwater and heat contents

Salinity is one of the best conserved quantities in the ocean, because there is no salt exchange between the ocean surface and the atmosphere. Therefore the change in salinity S results directly from the freshwater added to, or extracted from, the observed water body with a chosen reference salinity S_{ref}. In this study the reference salinity is chosen to equal the mean salinity of Fram Strait outflow, 34.9, which is also close to the mean salinity of the upper Polar Deep Water (Rudels et al., 1994) and can therefore be seen as the salinity at the depth of 1000 dbar above which the freshwater content is studied. Relative freshwater content FWC is given by

$$\mathrm{FWC} = \int_{z_1}^{z_2} \frac{S_{\mathrm{ref}} - S(z)}{S_{\mathrm{ref}}} \mathrm{d}z \tag{1}$$

which yields freshwater content as metres in a water column with horizontal cross-section of 1 m^2. The upper z_1 and lower z_2 vertical limits for each water mass are defined as described in Sect. 2.3. The CTD-data give salinity S as 1 or 2 dbar averages which, with a good approximation (1 dbar = 0.99 m), equals 1 (2) m in the upper 1000 dbar and from here on pressure and depth are considered interchangeable. Thus dz = 1(2) m and the integration is replaced by summation over the limits of the layer.

Similar to the freshwater content, also the heat content is defined as a relative quantity. Here the choice of reference temperature θ_{ref} is set to –1.9 °C, which is slightly below the typical freezing point temperature in the Nansen Basin. The highest surface salinities, roughly 34.2, are observed in the Nansen Basin and therefore also the corresponding freezing point temperature, –1.88 °C, is the lowest. Consequently the choice of reference temperature yields the heat available for potential ice melt. The reference temperature is the same in all the discussed sub-domains although salinity and thus also the freezing point temperature have large spatial variability in the Arctic Ocean.

OSD
9, 2621–2677, 2012

The heat content Q is given by

$$Q = c_p \int_{z_1}^{z_2} \rho(z) \Delta\theta \mathrm{d}z \tag{2}$$

where the specific heat capacity c_p equals $3985\,\mathrm{J\,kg^{-1}\,K^{-1}}$ for seawater at salinity 35, temperature $\theta = 0\,^\circ\mathrm{C}$ and at the surface pressure. The potential density ρ (referenced to surface) is computed from the data acquired from the hydrographic observations. $\Delta\theta$ is the difference between $-1.9\,^\circ\mathrm{C}$ and the observed potential temperature.

2.5 Approach to seasonal ice melt

The icebreaker expeditions in the Arctic Ocean are commonly conducted close to the end of the melt season, between July and September, when the seasonal ice melt can add up to 2 m to the freshwater content in the water column. Because of its seasonal nature, the ice melt represents a challenge since it should be distinguished from the permanent freshwater content in the Polar Mixed Layer. During winter brine rejection induces convection that mixes the meltwater below the summer halocline, homogenising the vertical temperature structure in the Polar Mixed Layer. The seasonal ice melt decreases the salinity from that of winter homogenisation and therefore, following Rudels et al. (1996), all salinities less than the salinity at the depth of temperature minimum are assumed to result from melting as illustrated in Fig. 4.

Meltwater content MWC is computed in a way similar to the freshwater content, substituting the constant reference salinity S_{ref} of 34.9 in Eq. (1) with salinity S_{m} at the depth of temperature minimum. The salinity of the temperature minimum varies spatially and is determined separately from each CTD-cast. The actual freshwater content in the Polar Mixed Layer is computed using the chosen reference salinity $S_{\mathrm{ref}} = 34.9$ and treating the layer as if it was at a constant salinity S_{m}, which equals the reference salinity for meltwater. The integrated area from the salinity profile is then reduced

OSD
9, 2621–2677, 2012
Time and space variability of freshwater content
M. Korhonen et al.

to a simple rectangle that has an area defined with the difference between reference salinity and the salinity at the temperature minimum multiplied by the depth of the Polar Mixed Layer (Fig. 4).

To validate the method used to distinguish meltwater from the freshwater content in the Polar Mixed Layer the meltwater content estimated from hydrographic data is compared to the heat input during summer. The heat input during melt season is provided by NCEP/NCAR reanalysis surface fluxes (Kalnay et al., 1996) including the net shortwave radiation q_{sw}, the net longwave radiation q_{lw} as well as the sensible q_s and latent q_l heat fluxes (all quantities given in $\mathrm{W\,m^{-2}}$).

The cumulative heat flux q is integrated (Eq. 3) from the end of May (150th calendar day) to late August (240th calendar day).

$$q = \int_{150}^{240} (q_{sw} + q_{lw} + q_s + q_l)\mathrm{d}t \tag{3}$$

The beginning of the integration is chosen well after the beginning of the actual polar day in late March, since the ice is not initially at freezing point temperature and is required to warm up before the melt begins. The chosen date is still a couple of weeks in advance of that observed by Rigor et al. (2000) and Perovich et al. (2003) who reported that the surface melt did not begin until mid June. The integration also terminates some weeks prior to the end of melt season. However, the early closing date for the integration is determined by the timing of the ship-based CTD surveys, generally conducted in late August or early September (Table 1). Spatial integration of heat input is approximated within the area enclosing the hydrographic stations marked in Fig. 1. For each studied sub-domain average heat input ($\mathrm{J\,m^{-2}}$) is computed over a constant area regardless of the interannual mismatch between the locations of ship-based CTD sampling. This is not considered to cause critical error since the onset of melt and freeze-up occur simultaneously over large (hundreds of kilometres) length scales (Rigor et al., 2000).

OSD
9, 2621–2677, 2012

Assuming that all the heat received between June and August is consumed in the melting process and no heat is needed to warm the ice or transmitted through the ice into the upper ocean, the heat input q computed in Eq. (3) is further converted into the maximum possible ice melt in metres MWC in a water column with horizontal cross-section 1 m^{-2} by

$$\mathrm{MWC} = \frac{q}{L_{\mathrm{ice}} \cdot \rho} \tag{4}$$

where $L_{\mathrm{ice}} = 333.15\,\mathrm{kJ\,kg^{-1}}$ is the latent heat of ice and ρ is density of water. The density of water is used instead of the density of ice to give the height of a liquid water column which is comparable to the hydrographic meltwater estimate given by Eq. (1).

2.6 Caveats in data analysis

Compared to the present-day well-calibrated instruments the subjective choice of temperature minimum represents a considerably larger uncertainty than the measurement inaccuracies, typical errors for temperature and salinity being 0.001 °C and 0.002, respectively. Already in Fig. 3 the ambiguity in defining the temperature minimum is encountered. Compared to the casts obtained in the middle of the sub-basins defining the temperature minimum becomes even more complicated when approaching the rims of the Canada Basin. Close to the Bering Strait Alaskan Coastal Water and Bering Sea Summer Water deliver warm water directly beneath the Polar Mixed Layer and may occasionally lift the temperature minimum from its original position closer to the surface. Another local feature in the Canada Basin, particularly in the areas with heavy seasonal ice melt such as the Chukchi Borderlands and Southern Beaufort Sea, is the near surface temperature maximum resulting from warming of surface waters during summer. Because of increased stability near the surface, temperature minimum indicating the depth of winter convection is located between the near surface temperature maximum, defined with salinity below 30 or 31 and located around depth 20–35 m (Shimada et al.,

OSD
9, 2621–2677, 2012

2001; Jackson et al., 2010) and the temperature maximum originating from the ACW (S ~31.5) or BSSW (S ~32.5) at the depth 40–70 m (Fig. 3).

The difficulties to automatically detect the appropriate temperature minimum represent a limit to the sheer number of CTD casts used in this study, as each temperature minimum is visually determined. Despite the careful examination of hydrographic data, occasionally the definition of the temperature minimum is open for subjective interpretation and becomes a vague guess. Overall, the average depth of the temperature minimum defined here is suggested to be prone to underestimation due to the entrainment of oceanic heat stored below the Polar Mixed Layer.

Because of the upper limit of the CTD observations part of the hydrographic data is missing or of questionable quality near the surface. The conventions regarding the upper limit vary interannually, the uppermost observations sometimes obtained as deep as 10 dbar. Thereby, for better comparison, salinity and temperature are extrapolated as constant up to the surface from the value at 10 dbar regardless of the data quality near the surface. Generally the upper 10–15 dbar is fairly well homogenised by mechanical mixing and the error resulting from the extrapolation is negligible. In the Nansen Basin, where the vertical salinity gradient is weak close to the surface (see e.g. Fig. 3), the typical underestimation amounts to 1–2 cm of meltwater. This is generally the case also in the less saline Canada Basin. However, the findings of this study suggest that the recent freshening and warming add to the surface stability and no clear summer mixed layer is necessarily present at the time of observations: during 2008 on average 10–20 cm of meltwater is lost due to the extrapolation.

In addition to the definition of temperature minimum and the extrapolation of data particularly the meltwater content is exposed to multiple caveats. The method used here is not able to distinguish river runoff, accounting for lower salinities than the salinity at the base of Polar Mixed Layer, from the actual seasonal ice melt. This may cause large overestimations near the continental slopes. Furthermore, the oceanographic observations obtained by the icebreakers are biased towards waters with low ambient ice concentration, implying higher than average ice melt. On the other hand part of the

OSD
9, 2621–2677, 2012

meltwater is out of reach of the oceanographic observations because of basal melting beneath the thicker ice floes and also the large melt pools on top of the sea ice. When the melt season is close to its end, the melt water on top of the ice floes has a high probability to be released to the ocean and hence increase, perhaps dramatically, the meltwater content in a short time. Thus, although all the icebreaker expeditions are conducted towards the end of the melt season, July–September, the two month difference between observations can have a significant effect on the meltwater content.

Although the combined error represented by the various uncertainties is largest for the meltwater content, the extrapolation of temperature influences also the heat content close to the surface. For the heat content, the extrapolation of a constant temperature is a reasonable approximation in most of the Arctic as the warming is modest and most of the solar insolation is eventually used to melt sea ice. Here again, this estimate represents the largest caveat in the Canada Basin, where recent sea ice loss has enabled the solar radiation to warm the surface waters. Thus the average upper layer temperature is likely to be underestimated.

3 Results

3.1 Water mass analysis

It is essential first to address how the volumes of the different water masses vary in time and space, because the freshwater and heat contents as well as the water masses are defined with salinity and temperature and the freshwater and heat contents are prone to reflect the shift in the depth of isolines.

3.1.1 The upper halocline

The most substantial geographic disparities in the distribution of water masses in the Arctic Ocean derive from the distinct properties of the inflowing Atlantic and Pacific waters. This is especially evident for the upper halocline: since the upper halocline largely

OSD
9, 2621–2677, 2012

derives from the Pacific waters its thickness in the Canada Basin typically reaches over 150 m, whereas in the Eurasian Basin its thickness is reduced to roughly 20 m (Fig. 5). In the Nansen Basin the upper halocline is generally absent.

During the first half of the 1990s the upper halocline weakened considerably, from over 30 m to less than 10 m, in the Amundsen Basin. This so-called retreat of the Arctic halocline, due to the eastward advection of the shelf waters, reported in several studies (e.g. Morison et al., 1998; Steele and Boyd, 1998) is well documented in Fig. 5f. Figure 5d and e indicate that the thickness of the upper halocline was also reduced over the Lomonosov Ridge and in the Makarov Basin, from roughly 40 m to 20 m. However, the data from 1996 and 2001 have quite poor coverage in the Makarov Basin (Table 1) concentrating close to the Lomonosov Ridge (Fig. 1) and thus the magnitude of the reduction cannot be regarded representative for the whole basin.

After the drop in the AO index in the mid 1990s, the discharge from the Eurasian continental shelf to the Amundsen and Makarov basins was restored, which can be perceived as the recovery of the upper halocline. This recovery has previously been reported by Björk et al. (2002) and Boyd et al. (2002). Although a clear thickening is occurring also over the Gakkel Ridge and in 2005 and 2011 a thin upper halocline appears locally even in the Nansen Basin (not visible in average values presented in Fig. 5h), the upper halocline merely rebounds to its state in the early 1990s. A more substantial thickening is seen in the northern parts of the Canada Basin and over the Alpha-Mendeleyev Ridge (Fig. 5b and c). However, it should be acknowledged that the cruise tracks from 1990s and 2000s differ from one another in both these domains: the 1990s data are obtained west of the Chukchi Plateau and over the Mendeleyev Abyssal Plain, where the influence of Pacific waters is known to be less pronounced (McLaughlin et al., 2004), whereas the 2000s data cover also the more Central Canada Basin and are concentrated to the Alpha Ridge. On the other hand, Rabe et al. (2011) reported that the most plausible deepening of the isohaline 34 occurred in the vicinity of the Chukchi Plateau whereas a slight shoaling was observed towards the Eastern Canada Basin. The more modest change observed in the Southern Canada Basin,

OSD
9, 2621–2677, 2012

despite the strengthening of the Ekman pumping, indicates that the strong presence of the waters in the upper halocline range in the Northern Canada Basin is likely to result from the relocation of the center of the Beaufort Gyre between 1990s and 2000s (Proshutinsky et al., 2009), now enabling northward distribution of freshwater.

3.1.2 The Polar Mixed Layer

Contrary to the upper halocline, the Polar Mixed Layer is generally thickest in the Eurasian Basin, where the average winter convection reaches deeper than 50 m, in the Nansen Basin deeper than 80 m (Fig. 5h). In the Canada Basin, the large freshwater flux adds to the buoyancy and consequently limits the depth of winter convection to roughly 35 m (Fig. 5a and b). Because of the definition of the Polar Mixed Layer its thickness is susceptible primarily to the surface stability, which, however, is also influenced by the atmospheric forcing. As the advection of low salinity surface waters and sea ice was altered in the late 1980s and early 1990s (Steele and Boyd, 1998; Rigor et al., 2002), the resulting salinification in the Eurasian and Makarov basins weakened the stability of the upper layers. Regardless of the absence of the low salinity shelf waters, generally contributing to the Polar Mixed Layer, the winter convection attained roughly the same depth as the homogenisation reached into the underlying water masses. Consequently the thickness of the Polar Mixed Layer was maintained. Over the Gakkel Ridge the winter convection in 1996 and 2001 reached ∼85 m, roughly 15 m deeper than during more neutral AO conditions. During the past decade the strengthening stability appears to have influenced mostly the Nansen Basin where the depth of winter convection was reduced by roughly 20 m compared to the 1990s.

3.1.3 The lower halocline, the Atlantic Water and the upper Polar Deep Water

During the 1990s the Atlantic layer shoals ∼35 m in the Amundsen and Makarov basins (Fig. 5d and f). The shoaling, resulting in decreasing thickness of the halocline waters, is comparable to the ∼40 m shoaling reported by Steele and Boyd (1998). The Atlantic

Discussion Paper | Discussion Paper | Discussion Paper | Discussion Paper |

OSD
9, 2621–2677, 2012

Time and space variability of freshwater content

M. Korhonen et al.

Water is depressed back to its state in the early 1990s as the advection of low salinity shelf waters is restored. However, in the Nansen Basin the zero-isotherm marking the upper boundary for the Atlantic Water continues to shoal during the 2000s, extending 50 m closer to the surface in 2007 than in 1991, at the expense of both the Polar Mixed Layer and the lower halocline (Fig. 5h). This shoaling appears more modest than the 75–90 m observed by Polyakov et al. (2010) along the Eurasian continental slope.

After the initial reduction in thickness over the Gakkel Ridge, the thickness of the Atlantic layer is nearly maintained, although its downward displacement is evident as the upper halocline thickens towards the Bering Strait. Consequently, the volume of the upper Polar Deep Water appears to diminish as the boundary between AW2 and UPDW, the isotherm 0 °C, is occasionally located below 1000 dbar. In Fig. 5 the presence of the upper Polar Deep Water in the uppermost 1000 dbar of a water column appears to be pronounced in the Makarov and Amundsen basins compared to the Nansen Basin. This compares favourably with the circulation of intermediate waters described by Rudels et al. (1994). The saline and warm Fram Strait inflow becomes bathymetrically steered along the Gakkel Ridge and circulates in the Nansen Basin whereas the waters modified in the Barents Sea, eventually reaching higher density than the waters originating in the Fram Strait branch and thus contributing to the formation of the upper Polar Deep Water, are confined to the Eurasian continental slope and hence able to bypass the Lomonosov Ridge in larger amounts than the warmer Atlantic Water.

3.2 Freshwater content

One of the most prominent features in the Arctic Ocean is the presence of strong horizontal salinity gradient between the Eurasian and Amerasian basins. The unequally distributed freshwater results from the different properties of inflowing Atlantic and Pacific waters, but the imbalance is further emphasised by the large river discharge to the Canada Basin (Anderson et al., 1994; Swift et al., 1997). In the Nansen Basin the major contributor to the freshwater content is the ice melt induced by the warm Atlantic inflow. As seen in Fig. 6, the most remarkable variability in salinity in both time and space occurs in the Polar Mixed Layer and the upper halocline. In the deeper layers not only variability but also the standard deviation become virtually negligible.

The salinity variability is, by definition, reflected in the freshwater content. Figure 7 demonstrates how the freshwater content (relative to salinity 34.9) varies from roughly 3 m in the Nansen Basin to 20 m in the Southern Canada Basin. The most substantial increase occurs over the Alpha-Mendeleyev Ridge as the freshwater content is doubled between the Makarov Basin and the Northern Canada Basin. Although the thickness of the Polar Mixed Layer in the Canada Basin is less than half of that in the Nansen Basin (Sect. 3.1.2), the freshwater storage increases from the Nansen Basin to the Canada Basin as seen in Fig. 7, reflecting the rapid decline in the salinity of the PML (Fig. 6). Nevertheless, the upper halocline stands out as the largest freshwater reservoir in the Canada Basin, containing plausibly over half of the local freshwater content. In the Makarov and Eurasian basins the Polar Mixed Layer becomes the main storage for freshwater, containing about half of the total freshwater content.

In addition to the large space variability, also the most substantial time variability of freshwater content occurs in the two uppermost water masses. The decreasing freshwater content in the Polar Mixed Layer and in the upper halocline during the early 1990s, particularly evident in the Amundsen and Makarov basins, is associated with the highly positive AO index changing the pathways of Siberian river runoff. In the Amundsen and Makarov basins the upper halocline freshwater content diminishes primarily due to its reduced thickness (Fig. 5) although the salinity increase from roughly 33.5 to 34 (Fig. 6) is also a significant contributor. In the Polar Mixed Layer the reduction in freshwater content results solely from its increasing salinity. The salinification of the Polar Mixed Layer is deduced to result from the intensified export of liquid freshwater (Karcher et al., 2005) and sea ice (Vinje, 2001) through the Fram Strait. Furthermore the divergence of the Arctic sea ice cover created open leads and increased heat loss from the open ocean (Rigor et al., 2002), subsequently enabling rapid freezing and brine rejection. This further increased the salinity of the upper layers in the Arctic Ocean.

OSD
9, 2621–2677, 2012

According to Boyd et al. (2002), the surface salinity in the Nansen, Amundsen and Makarov basins continued to increase until 1998. Despite the fact that this year falls into a gap in the data sets used in this study, the observations from 1996 and 2001 support this result and suggest that the salinification ceases in the late 1990s. After the advection of low salinity shelf water from the Eurasian continental shelf into the Makarov and Amundsen basins is re-established and the upper halocline recovered, most of the variability in freshwater content takes place in the Polar Mixed Layer. While the salinity of the upper halocline appears to rebound towards the pre-1990s values, the freshening of the Polar Mixed Layer is more pronounced despite its large interannual variability. However, the strong presence of the upper halocline over the Gakkel Ridge and its appearance in some of the stations obtained from the Nansen Basin in 2005 and 2011 (not visible in Fig. 7h due to the averaging) is a noteworthy feature.

Interestingly, despite the freshening in the upper layers, the Nansen Basin remains the only domain where the total freshwater content rather declines than increases. During the 2000s the freshwater content in the lower Atlantic layer becomes more explicitly negative due to its large volume and a slight increase (0.01–0.02 ppt) in salinity (Figs. 4h and 5h). This saline pulse is not seen elsewhere in the Arctic Ocean; over the Gakkel Ridge even a slight freshening of the Atlantic layer is observed. Note that the negative freshwater content presented in Fig. 7h should be subtracted from the positive column in order to get the total freshwater content.

Despite the weakening of the Beaufort Gyre in early 1990s, freshwater content has been increasing nearly continuously in the Canada Basin during the past two decades. The most substantial increase seems to occur in the upper halocline in the Northern Canada Basin where the freshwater content increased from roughly 3–4 m in 1990s to 8–9 m in 2008 and 2011. Also over the Alpha-Mendeleyev Ridge the upper halocline gains an additional 3–4 m of freshwater by the end of 2000s. Regardless of the mismatch in the locations of the data sets from 1990s and 2000s, the observed increase in the Northern Canada Basin and Alpha-Mendeleyev Ridge compares well with the results by Rabe et al. (2011) who, analysing a much more extensive data set, reported an

OSD
9, 2621–2677, 2012

increase of 3–4 m for the central part of the Northern Canada Basin between periods 1992–1999 and 2006–2008. According to Rabe et al. the freshwater content around the Chukchi Plateau increased even more, by 8 m.

Compared to the results of Rabe et al. (2011) the interannual variability of freshwater content in the Southern Canada Basin remains rather modest. Rabe et al. suggested an up to 8 m increase in FWC in the Central Beaufort Sea. However, near the basin margins they found negative change, possibly due to the upwelling induced by the intensified Ekman transport. Here the freshwater content of the upper halocline appears to remain close to 12 m – only exception being year 2002 when the data sampling concentrated in the vicinity of the Chukchi Plateau and the freshwater content appears to become substantially reduced. The slight freshening in the Polar Mixed Layer corresponds primarily to the decrease in salinity, from 29.12 in 2002 to 28.62 in 2008 (Fig. 6a). Comparison with the data obtained in the 1990s proves difficult: the highest mean salinity, 29.55, is observed in 1993, whereas the lowest salinity, 28.32, is observed in 1997. The low salinity in 1997 is likely to indicate the strong presence of Mackenzie discharge reported by Kadko and Swart (2004). The fresh waters deriving from the Mackenzie could also explain the high standard deviation of that year.

Proshutinsky et al. (2009) suggest that the freshening in the Beaufort Sea during the past decade was mainly confined to the Polar Mixed Layer while the freshwater content of the Pacific derived waters, here studied as part of the upper halocline, was rather decreasing. Regardless of the different methods in defining the Polar Mixed Layer, Proshutinsky et al. are using the isohaline 31 instead of the depth of winter convection, the data available for this study also exhibit more pronounced freshening in the Polar Mixed Layer (by ~1 ppt) than in the upper halocline, where the salinity decrease is an order of magnitude smaller. The decrease in the PML salinity in the Southern Canada Basin corresponds to roughly 1 m increase in freshwater content (Fig. 7a), which could result from the recent sea ice loss.

OSD
9, 2621–2677, 2012

3.3 Heat content

A significant amount of the heat residing in the Arctic Ocean is stored in the Atlantic layer. Part of the heat carried by the Atlantic inflow is used to melt ice or is lost to the atmosphere after it enters the Nansen Basin. Beyond the Nansen Basin the heat loss to the atmosphere is reduced due to increased freshwater storage and stability and the consequent downward displacement of the Atlantic Water. However, a more important cause behind the reduction in heat content over the Gakkel Ridge may be the different properties of the two inflow branches, through the Fram Strait and Barents Sea (Schauer et al., 1997), and their distribution within the Arctic Ocean.

Changes in both thickness (Fig. 5) and temperature (Fig. 8) are reflected in the time and space variability of heat content (Fig. 9) in the Atlantic layer. Beyond the Nansen Basin the thickness of the Atlantic layer is reduced as the colder upper Polar Deep Water gains volume as discussed in Sect. 3.1. The drop in temperature can easily be perceived from Fig. 8: in the Nansen Basin the Atlantic Water has an average potential temperature of 1–2 °C, the upper part (AW1) being considerably warmer than the lower layer (AW2), whereas over the Gakkel Ridge the temperature of AW1 is roughly 1 °C, AW2 well below that. Even in the Amerasian Basin, where the temperature difference between the two layers decreases, the Atlantic layer maintains an average temperature of 0.5 °C.

Although the space variability is damped beyond the Nansen Basin, the anomalously warm Atlantic inflow in 1990 reported by e.g. Quadfasel (1991) and Carmack et al. (1995) intrudes as far as the Makarov Basin, rising temperatures by 0.5 °C by 1996 (Fig. 8d). The weakened signal reaches the Canada Basin by 2002 when the average temperature increases by 0.2 °C, somewhat less in the lower and more in the upper Atlantic layer (Fig. 8a and b). This is comparable with the 0.25 °C warming of the Atlantic core observed north of the Chukchi Plateau in 2002 by McLaughlin et al. (2009), who examined the arrival and spreading of the warm Atlantic anomaly with more extensive and frequent observations. Furthermore, McLaughlin et al. noted that it took five years for the warm signal to penetrate into the interior of the Canada Basin. The oceanographic data analysed here suggests that the warming of the Atlantic layer in the Central Canada Basin is still ongoing in 2008.

Only in the Nansen Basin does the heat content continue to increase during the 2000s. By 2005 the average temperature of upper Atlantic Water (AW1) reaches 2 °C, exceeding the temperature in 1991 by almost one degree (Fig. 8h). The temperature of AW1 stays high in 2007 while the lower Atlantic layer is still slightly warming. Also the warming of the lower Atlantic Water layer (AW2) is evident although not as vigorous as in AW1. Nevertheless, despite its slower warming, the heat content increase is more pronounced in AW2 due to its increasing volume (Figs. 4h and 9h). After 2007 the warming ceases in both Atlantic layers and by 2011 the temperatures drop close to the values in the late 1990s.

Remarkably, despite the warmer boundary flow along the Eurasian continental slope observed in 2004 by Polyakov et al. (2005), the upward trend in the Atlantic heat transport during the 2000s has only a weak signal beyond the Nansen Basin. On the contrary, elsewhere in the Arctic Ocean the Atlantic layer temperature appears to decrease toward its state in the early 1990s. Thus it appears possible that the warm signal detected by Schauer et al. (2004), originating in the Fram Strait inflow, mainly recirculates in the Nansen Basin. It has already been suggested by Karcher et al. (2003) that only under favourable conditions, such as strong cyclonic circulation prevailing from the late 1980s to the mid 1990s, is a substantial amount of Fram Strait branch water able to cross the Lomonosov Ridge. Since the Barents Sea branch water is modified in the shallow Barents Sea through heat loss, ice melt and river runoff, the changes in the Atlantic inflow properties originating in the Nordic Seas do not necessarily exhibit a clear signal in the Arctic Ocean. Therefore it is likely that the Atlantic Water spreading into the Amerasian Basin across the Lomonosov Ridge during the 2000s derives mainly from the Barents Sea inflow. Not until 2007 does a slight warming indicate that the weakened signal deriving from the Fram Strait branch is spreading into the Amundsen

OSD
9, 2621–2677, 2012

Basin, reaching the Makarov Basin and the Alpha-Mendeleyev Ridge by 2011 (Fig. 8d, e and f).

Then why is the temperature in the upper Atlantic layer increasing more strongly than in the lower AW? Does not the retreating upper halocline enable more heat to be transferred to the upper ocean and eventually to the sea ice and the atmosphere? In the early 1990s it appears that most of the heat deriving from the North Atlantic is well preserved in the Atlantic layer and not mixed upward. On the contrary a possible cooling is observed in the lower halocline in the Eurasian and Makarov basins (Fig. 8). It is also remarkable that regardless of the underlying warm Atlantic Water, the lower halocline temperature is at lowest, below –1 °C, in the Nansen Basin. The low temperature indicates that the winter haline convection is deep enough to reach down into the thermocline and to replace part of the halocline with surface water that is cooled to the freezing point temperature. As earlier discussed by Kikuchi et al. (2004) and Rudels et al. (2004) during the 1990s the significance of local convection in the Arctic Ocean in forming halocline waters was emphasised due to the absence of advection from the continental shelves.

In the 2000s the negative correlation between Atlantic and lower halocline temperatures in the Amundsen and Makarov basins goes on as the temperatures of both layers appear to rebound back toward the values in the early 1990s. Also in the Nansen Basin cooling of the lower halocline ceases, presumably due to the slight freshening of the surface layers and the increased stability. The large standard deviation in the data obtained in 2005 should be noted since that year the Nansen Basin data consist of only two casts, of which the one taken immediately north of the Svalbard exhibits anomalously high average temperature (1.25 °C) in the lower halocline.

Regardless of the decreasing heat content of the lower halocline in the Eurasian and Makarov basins during the 1990s, no warming of the upper halocline or the Polar Mixed Layer is observed (Figs. 8 and 9). Hence the heat from the lower halocline is presumably lost directly to atmosphere (see also Sect. 3.4 for the influence of the oceanic heat flux on seasonal ice melt). Even the significance of the slight warming

OSD
9, 2621–2677, 2012

of the Polar Mixed Layer during the 2000s in the Northern Canada Basin and over the Alpha-Mendeleyev Ridge should be considered together with the freshening of the surface water presented in Fig. 6 as the freezing point temperature depends on the local salinity. This is reflected also to the temperature of the Polar Mixed Layer since with lower salinity the freezing occurs at higher temperatures and the water mass cannot be cooled below that temperature during winter; consequently the temperature in the beginning of the summer is initially higher, likely yielding higher temperatures at the end of the melt season. Moreover, it should be acknowledged that the apparent horizontal variability in the heat content of the uppermost two layers results from the constant reference temperature. The chosen reference temperature, –1.9 °C, is close to the freezing point temperature in the Nansen Basin, generally yielding a negligible heat content for the Polar Mixed Layer. On the other hand, for the relatively low salinity surface waters in the Canada Basin, the chosen reference temperature is considerably lower than the local freezing point temperature, –1.6 °C corresponding to the mean salinity 29 in the Polar Mixed Layer (Fig. 6a). In a 35 m thick layer (Fig. 5a) the heat content is reduced by 1/4 when the reference temperature of 1.6 °C is used instead of 1.9 °C. Since the dominant water mass in the upper halocline is the Bering Sea Winter Water, which is formed in freezing processes, the constant reference temperature is also reflected in the upper halocline heat content.

No substantial variability in the upper halocline temperature is observed and the primary cause behind the time variability of the upper halocline heat content is the changes in its thickness (compare e.g. Figs. 5b and 9b). Because the upper halocline is defined here to consist of all three water masses deriving from the Bering Strait (ACW, BSSW, BSWW), the possible warming of any of these water masses, suggested by Shimada et al. (2006) and Woodgate et al. (2010), cannot be assessed separately. In the Southern Canada Basin, where the changes in heat flux from the Pacific Ocean are expected to be the most striking, the temperature rather appears to decrease. However, the possible warming of ACW or BSSW could be overshadowed out by the Bering Sea Winter Water, which has an average temperature barely above the freezing

OSD
9, 2621–2677, 2012

point (Fig. 8). Moreover, the additional heat imported through the Bering Strait could be consumed by ice melt, or lost to the atmosphere, already over the shallow marginal seas.

In addition to the advection of warm waters from the Pacific Ocean, the marginal seas receive heat from the atmosphere due to their southern location. Consequently the summer ice concentration is typically lower over the shelves than in the central basins. This enhances the difference in surface temperatures between the shelves and the ice covered deep basins. Particularly in the Southern Canada Basin the large standard deviations of the Polar Mixed Layer temperatures shown in Fig. 7a are suggested to be due to the advection of the warm waters from the shelves. For example the hydrographic data obtained from the southernmost Beaufort Sea during the Henry Larsen 1993 expedition exhibit a core of anomalously warm (>5 °C) water close to the surface (maximum temperature around 22–24 m). This pool of warm water, suggested by Carmack et al. (1995) to be related to the low ice concentration in the Bering and Chuckhi seas during that summer, increases the average potential temperature and the heat content considerably. As a result of large regional variability the possible warming of surface waters, attributable to the recent loss of sea ice and increased absorption of solar radiation, becomes hidden.

3.4 Meltwater

Following the results obtained by e.g. Maykut and McPhee (1995) the seasonal ice melt is here approached presuming that the solar insolation is the primary source of energy for the melt, oceanic heat becoming significant only over the shallow marginal seas. In Fig. 10 the potential seasonal ice melt induced by the atmospheric heat input (from the NCEP surface fluxes) is compared to the hydrographic melt estimate. The hydrographic estimate is the direct result from the method described in Sect. 2.5. However, depending largely on the ice concentration, part of the solar insolation becomes absorbed by the surface layer before it is consumed in basal and lateral melt. Therefore in Fig. 11 the heat still remaining in the Polar Mixed Layer at the time of observations (Fig. 9) is added to the heat required to induce seasonal ice melt estimated from the hydrographic data (Fig. 10). This hydrographic heat estimate is compared with the cumulative heat flux (same as that used to compute meltwater content presented in Fig. 10) obtained from the NCEP Reanalysis data.

Both methods for estimating the meltwater content, the hydrographic data and NCEP Reanalysis heat fluxes, suggest that the average annual melt adds 1–2 m to the freshwater content in the Polar Mixed Layer. The cumulative heat input indicates considerably less variability in seasonal ice melt than the hydrographic melt estimate. Based on the hydrographic estimate the lowest seasonal ice melt occurs in the Nansen Basin, where 0.1–1.1 m of meltwater is added to the surface layer annually. The meltwater content is roughly doubled in the Amundsen Basin (0.4–1.6 m) and in the Makarov Basin it reaches 0.6–2.8 m. The hydrographic melt estimate yields typically over 2 m of meltwater for the Southern Canada Basin. According to the heat input estimate only the Southern Canada Basin proves different from the other basins: there the heat input amounts to ~2.2 m of meltwater, comparing well with the hydrographic estimate, whereas in the other basins the potential ice melt induced by atmospheric heat fluxes is 1.5 m. The large atmospheric heat flux into the Southern Canada Basin results from its southern location and reduced ice concentration during summer.

According to the hydrographic estimates the largest interannual variability of meltwater content occurs in the northernmost domains, the Makarov Basin and the Lomonosov Ridge. Also the horizontal variability is largest in the vicinity of the North Pole, where the high standard deviation in 1994, 2005 and 2007 is due to a few stations indicating significantly higher than average melt (Fig. 10d, e and f). It is noteworthy that the suspiciously high melt in 2001 exhibits only modest standard deviation. Not solely the large meltwater content itself is remarkable, but also the timing is striking: the observations used to estimate the seasonal ice melt in 2001 are obtained in July – two months prior to the end of melt season and also one month earlier than the other expeditions (Table 1). Particularly for the seasonal ice melt, the interannual variability in the timing and location of observations presents difficulties in forming a comprehensive

OSD
9, 2621–2677, 2012

picture, although in this case the results appear to be rather contrary to what would intuitively be expected.

Besides the relatively low salinity observed in the Polar Mixed Layer in the Makarov Basin and over the Lomonsov Ridge the hydrographic melt estimate in 2001 is influenced by the strong stratification manifesting as steep salinity and temperature gradients directly above the temperature minimum (not shown). In addition the salinity at the base of Polar Mixed Layer, here used as a reference salinity to compute meltwater content, is relatively high in 2001. This high salinity may be a remnant from the salinification of the PML during the 1990s (Fig. 6d and e). Furthermore, the advection of meltwater from the adjacent areas in response to atmospheric forcing could partially explain the unusually large melt estimate in the Makarov Basin and over the Lomonosov Ridge. Thus the hydrographic melt estimates are likely to be influenced by local conditions and possibly reflect the ocean advection of heat and low salinity surface waters.

Regardless of the large time and space variability in the hydrographic melt estimate, on average the results obtained by the two distinct methods are in reasonable agreement. The highest correspondence is reached close to the North Pole, over the Lomonosov Ridge and in the Amundsen and Makarov basins. Therefore the individual melt maxima in 2001 and 2007 can be seen as exceptional local features emphasised by restricted spatial extent of the direct observations. Since the order of magnitude is the same, $10^8\,\mathrm{J\,m^{-2}}$, for the heat used and the heat potentially available for melt (Fig. 11), the approach to distinguish meltwater is considered reasonable. The results, at least from the Southern Canada Basin, also compare favourably with the annual heat input of $9.7 \cdot 10^8\,\mathrm{J\,m^{-2}}$ estimated by Perovich et al. (2007b): whereas the NCEP Reanalysis products yield the June–August cumulative heat input in the Southern Canada Basin to be roughly $7.5 \cdot 10^8\,\mathrm{J\,m^{-2}}$, the hydrographic estimate yields somewhat higher heat input into the ice-ocean system, $9 \cdot 10^8\,\mathrm{J\,m^{-2}}$ (Fig. 11a). This could indicate that the oceanic heat fluxes may become important in the Canada Basin.

Contrary to the situation in the Canada Basin, in the Nansen Basin the melt estimated from the hydrographic data, generally below 1 m, occasionally even below 0.5 m, is

OSD
9, 2621–2677, 2012

substantially lower than the potential ice melt of roughly 1.5 m determined from NCEP Reanalysis heat fluxes. Regardless of the difference the hydrographic melt estimate clearly reflects the interannual variability in atmospheric heat fluxes (Figs. 9h and 10h). Nevertheless, the difference between the two estimates is remarkable since, in addition to the atmospheric heat, the Polar Mixed Layer in the Nansen Basin is presumed to gain oceanic heat from the underlying Atlantic Water. Intuitively, this would imply higher melt than the estimate based solely on the atmospheric fluxes. A closer inspection of the temperature and salinity profiles (not shown) reveals that the warming of the Polar Mixed Layer from below and the consequent upward displacement of the temperature minimum does not significantly influence the hydrographic melt estimate due to the nearly constant salinity below the summer halocline, found notably closer to the surface than the approximated temperature minima. The low melt indicates that even weak stratification may inhibit mixing of Atlantic heat content close to the sea ice, rendering the sea ice better insulated than generally assumed. Based on the high salinity of the surface layer in the Nansen Basin Rudels (2010) suggested that the ice melt remains low despite the heat flux from below since up to 75 % of the heat provided from the Atlantic layer is lost to the atmosphere.

Among the large time variability of seasonal ice melt an almost persistent decreasing trend from 1991 until 1996 can be identified in large parts of the Arctic Ocean (Figs. 10 and 11). A wide-spread meltwater minimum is reached in 1996 in the Eurasian Basin as well as in the Makarov Basin. The decreasing meltwater content appears to result from the simultaneously diminishing net atmospheric heat input. This implies that regardless of the reported strong ice export (Vinje, 2001) and divergence (Rigor et al., 2002), which possibly reduced the ice concentration and consequently also the surface albedo, the increase in heat loss from the exposed ocean surface, or through thin newly formed ice, exceeded the additional absorption of incoming solar radiation into the ice-ocean system.

Since 2001 the atmospheric heat input increases everywhere in the Arctic Ocean. Nevertheless, in the Canada and Makarov basins, the heat input merely rebounds to its

OSD
9, 2621–2677, 2012

values in 1993 (Fig. 11a, b and d). A more substantial increase is seen in the Eurasian Basin (Fig. 11f, g and h). According to the National Snow and Ice Data Center the ice extent in 2011 exceeded only slightly the record minimum in 2007. However, in 2011 the ice retreat North of Eurasia was shifted westward, from the East Siberian Sea to the Laptev Sea, which resulted in higher than average meltwater content for example over the Lomonosov Ridge. Moreover, in the Nansen Basin the meltwater content, exceeding 1 m, is clearly higher than during the previous years. Although also the seasonal ice melt estimated from the NCEP heat fluxes shows an evident increase during the 2000s, the hydrographic melt estimate increases more forcefully, yielding a better agreement between the two estimates in the Makarov and Amundsen basins compared to the preceding decade (Fig. 10d, e and f).

Although the increase appears modest for the Canada Basin where the most dramatic ice loss has occurred, the hydrographic melt estimates throughout the observational period are high compared to the average seasonal melt of 1.2 m reported by McPhee et al. (1998) and Perovich et al. (2003). This is likely due to the fact that the observations are biased to the area of open ocean, for example leaving the eastern side with the thickest multiyear ice unsampled. Particularly the high meltwater content in both 1993 and 1997 may result from the limited access of icebreakers to the ice-covered areas: the hydrographic observations during the 1990s are restricted to the vicinity of North American continental slope where the Mackenzie discharge is likely to lower the salinity of the Polar Mixed Layer. This presumption is supported by Guay and Falkner (1997) who concluded, based on the dissolved barium concentration, that large amount of river discharge was present near the North American continental slope in 1993. Also in 1997 0.8 m of the freshwater content was traced by Kadko and Swart (2004) to originate in the Mackenzie discharge. This might result in the observed warm and low salinity (as low as 24) water at the depth of 20 m. Furthermore, it is likely that the seasonal ice melt in 1997 was in fact anomalously high: based on satellite imagery Kwok and Cunningham (2010) reported that prior to the 2000s a single extreme melt event of multiyear ice occurred in 1997.

OSD
9, 2621–2677, 2012

During the past decade the icebreakers were no longer restricted to the continental slopes and the horizontal data coverage increased as the retreating ice cover made the Central and Northern Canada Basin more accessible. However, two serious caveats emerge by the year 2008. First, the neglect of the low salinity surface layer, discussed in Sect. 2.6, underestimates the seasonal ice melt in the Southern Canada Basin by 10–20 cm. Secondly, the dramatic loss of ice cover in 2007 increased surface stratification and prevented the winter convection from reaching the near surface temperature maximum formed during the previous summer. Consequently part of the heat stored in the Polar Mixed Layer during 2007 was still present in summer 2008, making the near-surface structure more complex and representing even larger uncertainties to the estimated depth of the PML in 2008.

Unfortunately, the areal sea ice minimum recorded in 2007, largely due to the decline in the Western Canada Basin (Perovich et al., 2008), is not covered by the data sets available for this study. However, the meltwater content of approximately 2.8 m in the Makarov Basin is twice as high as the local average and likely to reflect the excessive melt during 2007. Comiso et al. (2008) suggested that persisting southerly winds pushed the anomaly in sea ice concentration northward. According to Wang et al. (2009) these winds also enhanced the inflow of warm Pacific waters between 2004 and 2007 and accelerated the Transpolar Drift Stream. Thus the northward advection of meltwater, sea ice and surface waters warmed by solar radiation may have contributed to the high melt estimate in the Makarov Basin. The advection could explain the horizontal variability resulting in the high standard deviation in the meltwater estimates in 2007.

The data obtained in 2008 reveal that the seasonal ice melt in the Southern Canada Basin reaches 2.7 m. Perovich et al. (2008) estimated that the basal melt in 2007 was 2.1 m and the surface melt near the average of 0.64 m in the Beaufort Sea. Thus the hydrographic estimate for seasonal ice melt in 2008 appears comparable with the 2007 high melt event. However, the melt estimate presented here exceeds the 2007 estimate by Perovich et al. and reaches nearly 3 m when including the neglected low

OSD
9, 2621–2677, 2012

salinity water in the upper 10 m (see Sect. 2.6). This agrees with Kwok and Cunnigham (2010) who reported that, compared to the areal minimum reached in 2007, the most excessive loss of sea ice volume occurred in 2008.

4 Conclusions

4.1 Heat sources for the ice melt

The results obtained in this study indicate that despite the continuously increasing heat content and the shoaling Atlantic layer in the Nansen Basin, the heat entrainment from below the haloclines is not significant for the upper ocean energy budget. This appears to be the case even in the Amundsen and Makarov basins where the retreating upper halocline during the 1990s was suspected to enhance the oceanic heat flux to the sea ice (Steele and Boyd, 1998; Martinson and Steele, 2001; Björk et al., 2002). Instead the intensified export (Vinje, 2001) and divergence (Rigor et al., 2002) of sea ice as well as the thinning ice cover appear to enhance the heat loss from the Polar Mixed Layer. This is seen as the decline in the heat available for melting (Fig. 11).

On the other hand the salinification, due to changes in ocean advection and rapid ice formation, weakens the stratification and deepens the winter convection during the 1990s. The cooling of the lower halocline (Fig. 8) with simultaneously increasing salinity (Fig. 6) indicates that the convection reaches the thermocline, replacing the warmer waters with colder, brine enriched waters. This also implies that while the advection from the shelves is reduced, the halocline is primarily formed by convection. Despite the deep reaching convection, the oceanic heat deriving from the thermocline does not seem to increase ice melt substantially as the seasonal ice melt remains rather low (Fig. 10). However, the oceanic heat may have reduced ice formation during the winter previous to the observations.

The lower halocline is cooling even in the Nansen Basin where the Atlantic layer is persistently warming. As no evident sign of warming of the Atlantic Water beyond the

OSD
9, 2621–2677, 2012

Nansen Basin is recognized, the warmer Fram Strait branch is suggested to mainly circulate in the Nansen Basin whereas the waters cooled over the Barents Sea spread farther into the Arctic Ocean along the Eurasian continental slope. Only during anomalous climate conditions, such as the strongly positive AO in the late 1980s and early 1990s, does the Fram Strait branch distribute waters into the Amundsen and Amerasian basins.

Not until the turn of the century, when the Atlantic heat content began to decrease in large parts of the Arctic Ocean, do the melt estimates indicate a modest increase. Simultaneously with the increasing seasonal ice melt the ongoing freshening, particularly that of the upper halocline, is enhancing the stability and reducing the heat loss from the lower halocline. Despite that the temperature of the lower halocline increased by ~0.2 °C during the 2000s in the Northern Canada Basin and over the Alpha-Mendeleyev Ridge, a more substantial increase in heat content occurred in the upper halocline. The heat was gained through the increasing volume while the temperature of the upper halocline remained near the freezing point. Because the Pacific waters contributing to the upper halocline (ACW, BSSW, BSWW) are studied together, a possible slight warming of the minor (ACW, BSSW) halocline waters may be unnoticed. However, the examination of the upper 100 m of a water column, selected profiles presented in Fig. 12, reveals no consistent increase in the development of the ACW (S ~31) temperature maxima. It is also possible that the heat imported by the Bering Strait inflow is consumed by ice melt or lost to the atmosphere already over the shallow Chukchi Sea.

Even if the upper halocline waters were plausibly warming it is likely that due to the simultaneously ongoing freshening of the Polar Mixed Layer the heat would become trapped in the halocline. This is supported by the sinking of the temperature maxima of the Alaskan Coastal Water below 80 m in 2008 (Fig. 12). Thus it is unlikely that even the amplified stress induced by the rapidly moving thin ice could enforce the mechanical mixing and deepen the winter convection down to the halocline waters as was suggested by Yang et al. (2004) and Shimada et al. (2006).

Throughout the observational period most casts from the deep Canada Basin exhibit such near surface temperature maxima (S <30, depth ~30 m) as were described by Shimada et al. (2001) and Jackson et al. (2010). However, no evident warming of the near surface temperature maximum (NSTM) is identified from the data used here. As seen in Fig. 12. the forming of the NSTM is still in progress at the time of observations in 2008. Although the NSTM appears to shoal from 1997 to 2005, the accelerating ice melt is simultaneously strengthening the stratification, insulating the temperature maximum from the sea ice and the atmosphere. Due to both freshening and reduced ice formation the heat stored in the near surface temperature maximum is not reached: not even the winter convection has eroded the NSTM formed during 2007 and it proves to remain present the following summer below the summer halocline at the depth of ~60 dbar (Fig. 12).

Although no explicit heat source emerges in the upper ocean from the hydrographic observations, the comparison of the two melt estimates reveals that the high melt occasions in 2001, 2007 and 2008, based on the hydrographic observations, appear more pronounced than the mere atmospheric fluxes would predict. Admittedly many of these maxima can be attributed to the inability of the method to distinguish ocean advection from local ice melt. However, in 2007 and 2008 the necessity for a small, approximately 40 W, oceanic heat source to account for the estimated melt arises in the Canada and Makarov basins. Furthermore, comparing the two decades included in this study, during the past decade the decadal average of the hydrographic estimate in the Makarov and Amundsen basins equals or exceeds the estimate based on the atmospheric heat input whereas in the 1990s the hydrographic estimates remained in average well below the estimated potential ice melt (Fig. 11d, e and f). However, the difference between the two estimates represented in Fig. 10 is small compared to the uncertainty in both estimates and a further study is needed to define the possible oceanic heat sources and their contribution to the observed ice melt.

OSD
9, 2621–2677, 2012

4.2 The physical causes behind recent freshening

Regardless of the poor coverage and sparse data sets in this study the recent changes in the freshwater content in the Arctic Ocean agree well with other studies using much larger data sets. Both the downward trend in the upper ocean freshwater content during the 1990s and the accumulation of freshwater during the 2000s are identified. While the 1990s salinification was plausibly explained by the joint effect imposed by the redistribution of shelf waters within the Arctic Ocean (e.g. Steele and Boyd, 1998), export of liquid freshwater (Karcher et al., 2005) and sea ice (Vinje, 2001) to the Nordic Seas and subsequent formation of first year ice (Rigor et al., 2002), the freshening during the past decade has been mainly attributed to the Ekman pumping and accelerated ice melt (Proshutinsky et al., 2009; Rabe et al., 2011).

Whereas Rabe et al. (2011) studied the uppermost ocean above the isohaline 34 as a whole and concluded the decreasing salinity to be the primary cause behind the recent freshening, here the distinction between the upper halocline and the Polar Mixed Layer reveals that the freshening of the two layers is driven by different processes. Comparing Figs. 4, 5 and 6 the freshwater content in the upper halocline appears to reflect primarily the changes in the layer thickness. For example in the Northern Canada Basin the salinity decreases from ~33.0 in the 1990s to ~32.6 in the later half of 2000s, which adds only 1 m of freshwater into a 100 m thick layer. Because the observed freshwater increase, 5 m, is substantially larger than the salinity decrease can account for, it is suggested that the freshwater, possibly from the Eurasian continental shelf, is accumulating through the enhanced Ekman transport. In addition also some anomalously large inflow events through the Bering Strait, discussed by Shimada et al. (2006) and Woodgate et al. (2010), possibly add to the freshwater content in the upper halocline.

Compared to the Northern Canada Basin a more modest depression of isohalines is observed in the Southern Canada Basin, where the intensified Ekman transport is known to have accumulated low salinity water to the upper ocean during the last decade (Proshutinsky et al., 2009). Intuitively it would be expected that the large transports through the Bering Strait would first influence the upper halocline in the Southern Canada Basin. Nevertheless, the variability in the Southern Canada Basin may be partially overshadowed by the enlarging Beaufort Gyre distributing freshwater northward during the 2000s whereas during the 1990s the area of the Beaufort Gyre was confined to the Southern Canada Basin (Proshutinsky et al., 2009).

In contrast to the upper halocline, the salinity of the Polar Mixed Layer is substantially decreasing: by ~0.5 ppt in the Southern and by ~1 ppt in the Northern Canada Basin during the 2000s. The decreasing salinity in the Polar Mixed Layer is primarily attributed to the recent sea ice loss and reduced ice formation, adding almost one metre to the local freshwater content. However, regardless of the consequently increasing stability, also the winter convection deepens by roughly 5 m during the 2000s, from roughly 33 m to 38 m. This is clearly more than the excess ice melt can account for and hence it is suggested that also the Ekman convergence accumulates over 0.5 m of freshwater, probably deriving from the low salinity shelf waters, into the Polar Mixed Layer.

It should be noted that the distinction of meltwater (Fig. 10) and freshwater (Fig. 7) makes the total freshwater content of 20 m in the Southern Canada Basin appear small compared to other studies, such as Proshutinsky et al. (2009) and Rabe et al. (2011), reporting the freshwater storage in the Beaufort Gyre to reach 25 m. The meltwater content, however, amounts at highest nearly 3 m. It should also be acknowledged that the meltwater, as it is defined here, represents only the ice melt during the past summer. Since the freshening increases buoyancy, the reduced thermodynamic growth of sea ice does not induce sufficiently deep winter convection to erode the stratification down to the temperature minimum formed during the previous winter. As the uppermost temperature minimum is chosen as the base of the Polar Mixed Layer, part of the meltwater is incorporated into the freshwater content of the upper halocline. This can be seen in Fig. 12 where the near surface temperature maximum from the previous summer is still present in 2008 – now below the temperature minimum and the summer halocline, thus defined to form part of the upper halocline.

The Makarov Basin – Lomonosov Ridge area is estimated to receive over 2 m of additional freshwater to the Polar Mixed Layer after the late 1990s, which cannot be attributed solely to the rather modest melt in the Eurasian Basin. A more likely cause behind the increased freshwater content in the PML is the advection from the continental shelves as the less dense waters are transported to the central basins close to the surface. This is supported by Jones et al. (2008) and Bauch et al. (2011) who, based on phosphate and phosphate to nitrate concentrations, reported a large river water fraction in the upper 50 m of the Makarov and Lomonosov basins in 2005 and 2007. Bauch et al. also suggested that the river input in 2007 was due to a discrete pulse rapidly transported along the enhanced Transpolar Drift Stream. Although the freshening seems continuous from 2001 to 2007, it is possible that the data sets used in this study does not separate two discrete pulses of shelf water in 2005 and 2007. Nonetheless, the freshwater content ceases its increase by 2011. Thus in the Eurasian Basin the advective processes, including also melting in the marginal seas, are assumed to regulate the freshwater balance in both the Polar Mixed Layer and the upper halocline. However, the higher than average seasonal ice melt in 2011 may be incorporated into the Polar Mixed Layer decreasing its salinity and increasing its freshwater content during the following year.

Acknowledgements. The research leading to these results has received funding from the European Union's Sixth and Seventh Framework Programmes: DAMOCLES (Developing Arctic Modelling and Observing Capabilities for Long-term Environment Studies, contract n° 018509, and THOR (Thermohaline circulation – at risk?), FP7/2007-2013) under grant agreement n° 212643. Reiner Schlitzer's Ocean Data View (http://odv.awi.de, 2012) was used for drawing the maps.

References

Aagaard, K. and Carmack, E. C.: The role of sea ice and other fresh water in the Arctic circulation, J. Geophys. Res., 94, 14 485–14 498, 1989.

Aagaard, K., Coachman, L. K., and Carmack, E. C.: On the halocline of the Arctic Ocean, Deep-Sea Res., 28, 529–545, 1981.
Anderson, L. G., Björk, G., Holby, O., Jones, E. P., Kattner, G., Koltermann, K.-P., Liljeblad, B., Lindegren, R., Rudels, B., and Swift, J. H.: Water masses and circulation in the Eurasian Basin: results from the Oden 91 expedition, J. Geophys. Res., 99, 3273–3283, 1994.
Bauch, D., van der Loeff, M. R., Andersen, N., Torres-Valdes, S., Bakker, K., and Abrahamsen, E. P.: Origin of freshwater and polynya water in the Arctic Ocean halocline in summer 2007, Prog. Oceanogr., 91, 482–495, 2011.
Björk, G., Söderkvist, J., Winsor, P., Nikolopoulos, A., and Steele, M.: Return of the cold halocline layer to the Amundsen Basin of the Arctic Ocean: implications for the sea ice mass balance, Geophys. Res. Lett., 29, 1513, 2002.
Björk, G., Jakobsson, M., Rudels, B., Swift, J. H., Anderson, L., Darby, D. A., Backman, J., Coakley, B., Winsor, P., Polyak, L., and Edwards, M.: Bathymetry and deep-water exchange across the Central Lomonosov Ridge at 88–89° N, Deep-Sea Res., 54, 1197–1208, 2007.
Bourgain, P., Gascard, J. C., Shi, J., and Zhao, J.: Large-scale temperature and salinity changes in the upper Canadian Basin of the Arctic Ocean at a time of a drastic Arctic Oscillation inversion, Ocean Sci. Discuss., 9, 2001–2038, 2012, http://www.ocean-sci-discuss.net/9/2001/2012/.
Boyd, T. J., Steele, M., Muench, R. D., and Gunn, J. T.: Partial recovery of the Arctic Ocean halocline, Geophys. Res. Lett., 29(14), 1657–1660, 2002.
Carmack, E. C., Macdonald, R. W., Perkin, R. G., McLaughlin, F. A., and Pearson, R. J.: Evidence for warming of Atlantic Water in the Southern Canadian Basin of the Arctic Ocean: results from the Larsen-93 expedition, Geophys. Res. Lett., 22, 1061–1064, 1995.
Coachman, L. K. and Barnes, C. A.: The contribution of Bering Sea water to the Arctic Ocean, Arctic, 14, 147–161, 1961.
Comiso, J. C., Parkinson, C. L., Gersten, R., and Stock, L.: Accelerated decline in the Arctic sea ice cover, Geophys. Res. Lett., 35, L01 703, 2008.
Dickson, R. R.: Long-term coordinated changes in the convective activity of the North Atlantic, Prog. Oceanogr., 38, 241–295, 1996.
Dickson, R. R., Rudels, B., Dye, S., Karcher, M., Meincke, J., and Yashayaev, I.: Current estimates of freshwater flux through arctic and subarctic seas, Prog. Oceanogr., 73, 210–230, 2007.

Jackson, J. M., Carmack, E. C., McLaughlin, F. A., Allen, S. E., and Ingram, R. G.: Identification, characterization, and change of the near-surface temperature maximum in the Canada Basin, 1993–2008, J. Geophys. Res., 115, C05 021, 2010.
Jones, E. P., Anderson, L. G., Jutterström, S., Mintrop, L., and Swift, J. H.: Pacific freshwater, river water and sea ice meltwater across Arctic Ocean basins: results from the 2005 Beringia expedition, J. Geophys. Res., 113, C12 8012, 2008.
Kadko, D. and Swart, P.: The source of the high heat and freshwater content of the upper ocean at the SHEBA site in the Beaufort Sea in 1997, J. Geophys. Res., 109, C01 022, 2004.
Kalnay, E., Kanamitsu, M., Kistler, R., Collins, W., Deaven, D., Gandin, L., Iredell, M., Saha, S., White, G., Woollen, J., Zhu, Y., Cheillab, M., Ebsuzaki, W., Higgins, W., Janowiak, J., Mo, K. C., Ropelewski, C., Wang, J., Leetma, A., Reynolds, R., Jenne, R., and Joseph, D.: The NCEP/NCAR 40-yr reanalysis project, Bull. Amer. Meteor. Soc., 77, 437–470, 1996.
Karcher, M. J., Gerdes, R., Kauker, F., and Köberle, C.: Arctic warming-evolution and spreading of the 1990s warm event in the Nordic Seas and the Arctic Ocean, J. Geophys. Res., 108, C2 3034, 2003.
Karcher, M. J., Gerdes, R., Kauker, F., Köberle, C., and Yashayaev, I.: Arctic Ocean change heralds North Atlantic freshening, Geophys. Res. Lett., 32, L21 606, 2005.
Kikuchi, T., Hatakeyama, K., and Morison, J. H.: Distribution of convective lower halocline water in the Eastern Arctic Ocean, J. Geophys. Res., 109, C12 030, 2004.
Kwok, R. and Cunningham, G. F.: Contribution of melt in the Beaufort Sea to the decline in Arctic multiyear sea ice coverage: 1993–2009, Geophys. Res. Lett., 37, L20 501, 2010.
Lindsay, R. W. and Zhang, J.: The thinning of Arctic sea ice, 1988–2003: have we passed a tipping point?, J. Clim., 18, 4879–4894, 2005.
Martinson, D. G. and Steele, M.: Future of the Arctic sea ice cover: implications of an Antarctic analog, Geophys. Res. Lett., 28, 307–310, 2001.
Maslanik, J., Serreze, M., and Barry, R.: Recent changes in Arctic summer ice cover and linkages to atmospheric circulation anomalies, Geophys. Res. Lett., 23, 1677–1680, 1996.
Maykut, G. A. and McPhee, M. G.: Solar heating of the Arctic mixed layer, J. Geophys. Res., 100, 24 691–24 704, 1995.
McLaughlin, F. A., Carmack, E. C., Macdonald, R. W., Melling, H., Swift, J. H., Wheeler, P. A., Sherr, B. F., and Sherr, E. B.: The joint roles of Pacific and Atlantic-origin waters in the Canada Basin, 1997–1998, Deep-Sea Res., 51, 107–128, 2004.

McLaughlin, F. A., Carmack, E. C., Williams, W. J., Zimmermann, S., Shimada, K., and Itoh, M.: Joint effects of boundary currents and thermohaline intrusions on the warming of Atlantic Water in the Canada Basin, 1993–2007, J. Geophys. Res., 114, C00A12, 2009.

McPhee, M. G., Stanton, T. P., Morison, J. H., and Martinson, D. G.: Freshening of the upper ocean in the Arctic: is perennial sea ice disappearing?, Geophys. Res. Lett., 25, 1729–1732, 1998.

Morison, J. H., Steele, M., and Andersen, R.: Hydrography of the upper Arctic Ocean measured from the nuclear submarine U.S.S. Pargo, Deep-Sea Res. I, 45, 15–38, 1998.

Perovich, D. K., Grenfell, T. C., Richter-Menge, J. A. Light, B., Tucker, W. B., and Eicken, H.: Thin and thinner: sea ice mass balance measurements during SHEBA, J. Geophys. Res., 108, 8050, 2003.

Perovich, D. K., Light, B., Eicken, H., Jones, K. F., Runciman, K., and Nghiem, S. V.: Increasing solar heating of the Arctic Ocean and adjacent seas, 1979–2005: attribution and role in the ice-albedo feedback, Geophys. Res. Lett., 34, L19505, 2007a.

Perovich, D. K., Nghiem, S. V., Markus, T., and Schweiger, A.: Seasonal evolution and interannual variability of the local solar energy absorbed by the Arctic sea ice-ocean system, J. Geophys. Res., 112, C03005, 2007b.

Perovich, D. K., Richter-Menge, J. A., Jones, K. F., and Light, B.: Sunlight, water, and ice: extreme Arctic sea ice melt during the summer of 2007, Geophys. Res. Lett., 35, L11501, 2008.

Polyakov, I. V., Beszczynska, A., Carmack, E. C., Dmitrenko, I. A., Fahrbach, E., Frolov, I. E., Gerdes, R., Hansen, E., Holfort, J., Ivanov, V. V., Johnson, M. A., Karcher, M., Kauker, F., Morison, J. H., Orvik, K. A., Schauer, U., Simmons, H. L., Skagseth, Ø., Sokolov, V. T., Steele, M., Timokhov, L. A., Walsh, D., and Walsh, J. E.: One more step toward a warmer Arctic, Geophys. Res. Lett., 32, 17605, 2005.

Polyakov, I. V., Timokhov, L. A., Alexeev, V. A., Bacon, S., Dmitrenko, I. A., Fortier, L., Frolov, I. E., Gascard, J.-C., Hansen, E., Ivanov, V. V., Laxon, S., Mauritzen, C., Perovich, D., Shimada, K., Simmons, H. L., Sokolov, V. T., Steele, M., and Toole, J.: Arctic Ocean warming contributes to reduced polar ice cap, J. Phys. Oceanogr., 40, 2743–2756, 2010.

Proshutinsky, A. Y. and Johnson, M. A.: Two circulation regimes of the wind-driven Arctic Ocean, J. Geophys. Res., 102, 12 493–12 514, 1997.

Proshutinsky, A., Krishfield, R., Timmermans, M.-L., Toole, J. M., Carmack, E. C., McLaughlin, F. A., Williams, W. J., Zimmermann, S., Itoh, M., and Shimada, K.: Beaufort Gyre fresh-

OSD
9, 2621–2677, 2012
Time and space variability of freshwater content
M. Korhonen et al.

water reservoir: state and variability from observations, J. Geophys. Res., 114, C00A10, 2009.
Quadfasel, D., Sy, A., Wells, D., and Tunik, A.: Warming in the Arctic, Nature, 350, 385, 1991.
Rabe, B., Karcher, M., Schauer, U., Toole, J. M., Krishfield, R. A., Pisarev, S., Kauker, F., Gerdes, R., and Kikuchi, T.: An assessment of Arctic Ocean freshwater content changes from the 1990s to the 2006–2008 period, Deep-Sea Res. I, 58, 173–185, 2011.
Rigor, I. G., Colony, R. L., and Seelye, M.: Variations in surface air temperature observations in the Artic, 1979–97, J. Clim, 13, 896–914, 2000.
Rigor, I. G., Wallace, J. M., and Colony, R. L.: Response of sea ice to the Arctic oscillation, J. Clim., 15, 2648–2663, 2002.
Roach, A. T., Aagaard, K., Pease, C. H., Salo, S. A., Weingartner, T., Pavlov, V., and Kulakov, M.: Direct measurements of transports and water properties through the Bering Strait, J. Geophys. Res., 100, 18 433–18 457, 1995.
Rothrock, D. A., Yu, Y., and Maykut, G., A.: Thinning of the Arctic sea-ice cover, Geophys. Res. Lett., 26, 3469–3472, 1999.
Rudels, B., Jones, E. P., Anderson, L. G., and Kattner, G.: On the intermediate depth waters of the Arctic Ocean, in: Polar Oceans and Their Role in Shaping the Global Environment, edited by: Johanessen, O. M., Muench, R. D., and Overland, J. E., Geophysical Monograph 85, American Geophysical Union, Washington, 33–46, 1994.
Rudels, B., Anderson, L. G., and Jones, E. P.: Formation and evolution of the surface mixed layer and halocline of the Arctic Ocean, J. Geophys. Res., 101, 8807–8822, 1996.
Rudels, B., Jones, E. P., Schauer, U., and Eriksson, P.: Atlantic sources of the Arctic Ocean surface and halocline waters, Polar Res., 23, 181–208, 2004.
Rudels, B.: Constraints on exchanges in the Arctic Mediterranean – do they exist and can they be of use?, Tellus Series A, 62, 109–122, 2010.
Schauer, U., Muench, R. D., Rudels, B., and Timokhov, L.: Impact of Eastern Arctic shelf waters on the Nansen Basin intermediate waters, J. Geophys. Res., 102, 3371–3382, 1997.
Schauer, U., Fahrbach, E., Osterhus, S., and Rohardt, G.: Arctic warming through the Fram Strait: oceanic heat transport from 3 yr of measurements, J. Geophys. Res., 109, C06026, 2004.
Schauer, U. (Ed.): The Expedition ARKTIS-XXII/2 of the Research Vessel ”Polarstern” in 2007, Reports on Polar and Marine Research, Alfred Wegener Institute for Polar and Marine Research, Bremerhaven, 579, 271 pp., 2008.

Schauer, U., Rabe, B., and Wisotzki, A.: Physical Oceanography during POLARSTERN Cruise ARK-XXVI/3, Alfred Wegener Institute for Polar and Marine Research, Bremerhaven, in press, 2012.

Shimada, K., Carmack, E. C., Hatakeyama, K., and Takizawa, T.: Varieties of shallow temperature maximum waters in the Western Canadian Basin of the Arctic Ocean, Geophys. Res. Lett, 28, 3441–3444, 2001.

Shimada, K., Kamoshida, T., Itoh, M., Nishino, S., Carmack, E. C., McLaughlin, F. A., Zimmermann, S., and Proshutinsky, A.: Pacific Ocean inflow: influence on catastrophic reduction of sea ice cover in the Arctic Ocean, Geophys. Res. Lett., 33, L08605, 2006.

Steele, M. and Boyd, T.: Retreat of the cold halocline layer in the Arctic Ocean, J. Geophys. Res., 103, 10 419–10 436, 1998.

Steele, M., Morison, J., Ermold, W., Rigor, I., Ortmeyer, M., and Shimada, K.: Circulation of summer Pacific halocline water in the Arctic Ocean, J. Geophys. Res., 109, 2027–2044, 2004.

Stigebrandt, A.: The North Pacific: a global-scale estuary, J.Phys. Oceanogr., 14, 464–470, 1984.

Stroeve, J., Holland, M. M., Meier, W., Scambos, T., and Serreze, M.: Arctic sea ice decline: faster than forecast, Geophys. Res. Lett., 34, L09501, 2007.

Swift, J. H., Jones, E. P., Aagaard, K., Carmack, E. C., Hingston, M., Macdonald, R. W., McLaughlin, F. A., and Perkin, R. G.: Waters of the Makarov and Canada basins, Deep-Sea Res. II, 44, 1503–1529, 1997.

Thompson, D. W. J. and Wallace, J. M.: The Arctic oscillation signature in the wintertime geopotential height and temperature fields, Geophys. Res. Lett., 25, 1297–1300, 1998.

Vinje, T.: Fram Strait ice fluxes and atmospheric circulation: 1950–2000, J. Clim., 14, 3508–3517, 2001.

Wang, J., Zhang, J., Watanabe, E., Ikeda, M., Mizobata, K., Walsh, J. E., Bai, X., and Wu, B.: Is the dipole anomaly a major driver to record lows in Arctic summer sea ice extent?, Geophys. Res. Lett., 36, L05706, 2009.

Woodgate, R. A., Weingartner, T., and Lindsay, R.: The 2007 Bering Strait oceanic heat flux and anomalous Arctic sea-ice retreat, Geophys. Res. Lett., 37, L01602, 2010.

Yang, J., Comiso, J., Walsh, D., Krishfield, R., and Honjo, S.: Storm-driven mixing and potential impact on the Arctic Ocean. J. Geophys. Res., 109, C04 008, 2004.

Zhang, Z. (Ed.): The Report of 2003 Chinese Arctic Research Expedition, China Ocean Press, Beijing, 229 pp., 2004.

OSD
9, 2621–2677, 2012

Table 1. The icebreaker expeditions offering the data for this study and a reference for additional information about instruments and their accuracy. Number of casts in each sub-basin as well as the areal coverage of the available casts (in parentheses) is shown.

Year	Month	Vessel	Reference	Nansen Basin	Gakkel Ridge	Amundsen Basin	Lomonosov Ridge	Makarov Basin
1991	Aug/Oct	Oden	Anderson et al. (1994)	4 (30 %)	3 (10 %)	13 (35 %)	5 (25 %)	3 (5 %)
1994	Jul/Aug	Louis S. St-Laurent	Swift et al. (1997)	3 (15 %)	–	3 (10 %)	3 (25 %)	8 (20 %)
1996	Aug	Polarstern	Schauer et al. (2002)	12 (20 %)	2 (10 %)	12 (20 %)	5 (40 %)	10 (25 %)
2001	Jul/Aug	Oden	Björk et al. (2002)	9 (35 %)	2 (10 %)	13 (35 %)	9 (25 %)	3 (5 %)
2005	Aug	Oden	Björk et al. (2007)	2 (15 %)	1 (10 %)	6 (15 %)	9 (25 %)	6 (20 %)
2007	Aug/Sept	Polarstern	Schauer et al. (2008)	18 (50 %)	9 (60 %)	9 (20 %)	6 (40 %)	10 (25 %)
2011	Aug/Sept	Polarstern	Schauer et al. (in press)	21 (40 %)	10 (50 %)	18 (35 %)	5 (25 %)	10 (30 %)

OSD
9, 2621–2677, 2012

Table 1. Continued.

Year	Month	Vessel	Reference	Alpha-Mendeleyev Ridge	North Canada Basin	South Canada Basin
1993	Aug/Sept	Henry Larsen	Carmack et al. (1995)	2 (10 %)	5 (10 %)	7 (20 %)
1994	Jul/Aug	Louis S. St-Laurent	Swift et al. (1997)	4 (40 %)	8 (15 %)	–
1997	Sept/Oct	Louis S. St-Laurent	McLaughlin et al. (2004)	–	–	12 (25 %)
2002	Aug/Sept	Polar Star	Woodgate et al. (2002)	10 (40 %)	24 (25 %)	10 (15 %)
2003	Aug/Sept	Xuelong	Zhang (2004)	–	13 (20 %)	18 (35 %)
2005	Aug	Oden	Björk et al. (2007)	5 (10 %)	5 (20 %)	8 (25 %)
2007	Aug/Sept	Polarstern	Schauer et al. (2008)	5 (25 %)	–	–
2008	Aug/Sept	Xuelong	Bourgain et al. (2012)	5 (10 %)	16 (50 %)	27 (55 %)
2011	Aug/Sept	Polarstern	Schauer et al. (in press)	8 (25 %)	5 (10 %)	–

Table 2. The definitions of water masses with salinity and temperature.

Water mass	Upper limit (z_1)	Lower limit (z_2)
Polar Mixed Layer (PML)	$p = 0$ dbar	$\theta = \theta_{min}$
Upper halocline (UHC)	$\theta = \theta_{min}$	$S = 34$
Lower halocline (LHC)	$S = 34$	$\theta = 0\,^{\circ}\mathrm{C}$
Upper Atlantic Water (AW1)	$\theta = 0\,^{\circ}\mathrm{C}$	$\theta = \theta_{max}$
Lower Atlantic Water (AW2)	$\theta = \theta_{max}$	$\theta = 0\,^{\circ}\mathrm{C}$
Upper Polar Deep Water (UPDW)	$\theta = 0\,^{\circ}\mathrm{C}$	$p = 1000$ dbar

OSD
9, 2621–2677, 2012

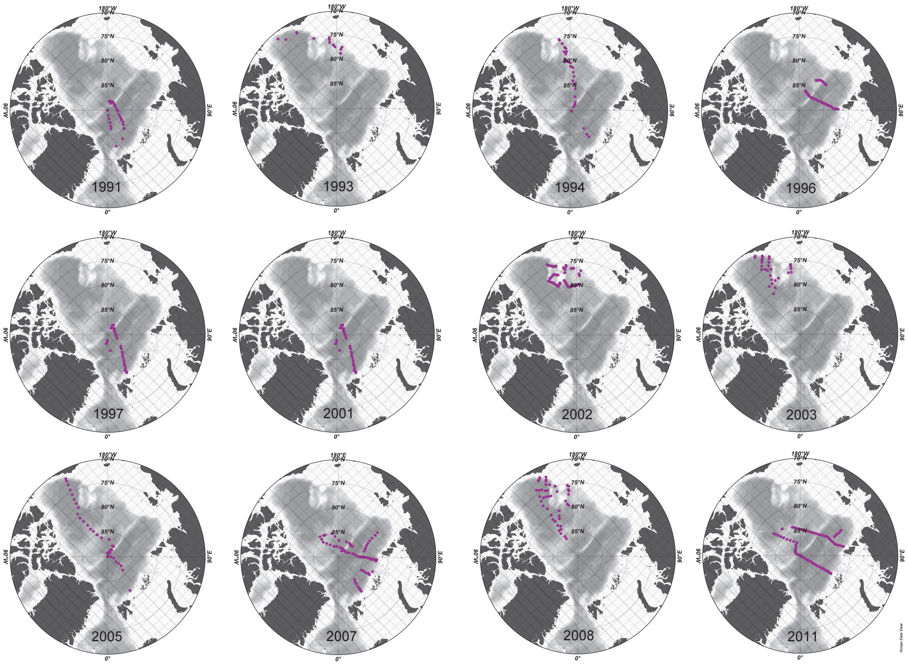

Fig. 1. The selected icebreaker cruises used in this study. The grid (approximately 1.8° × 1.8°) is used to compute areal coverages shown in Table 1. See Table 1 also for exact number of casts.

OSD
9, 2621–2677, 2012

Time and space variability of freshwater content

M. Korhonen et al.

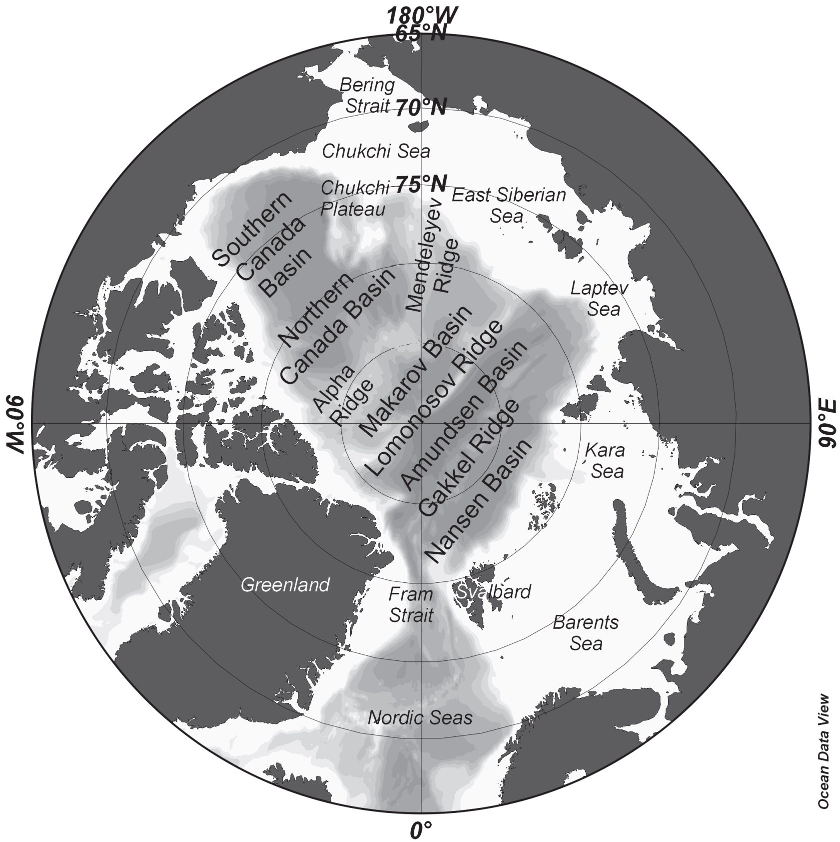

Fig. 2. The sub-basins and -ridges in the Arctic Ocean included in this study: Southern and Northern Canada basins, Alpha-Mendeleyev Ridge, Makarov Basin, Lomonosov Ridge, Amundsen Basin, Gakkel Ridge and Nansen Basin. Also other regions mentioned in the text are shown in italic.

OSD
9, 2621–2677, 2012

Time and space variability of freshwater content

M. Korhonen et al.

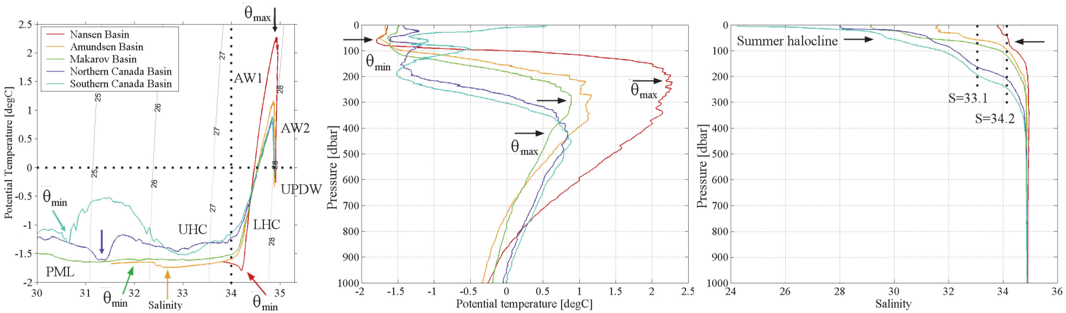

Fig. 3. The θS-diagram as well as the potential temperature and salinity profiles showing the definitions of water masses (PML = Polar Mixed Layer, UHC = upper halocline, LHC = lower halocline, AW1 = upper Atlantic Water, AW2 = lower Atlantic Water, UPDW = upper Polar Deep Water). The coloured arrows in the θS-diagram show the temperature minimum for each cast, the black arrow marks the temperature maxima. For the temperature profiles an approximate depth of the temperature minima is indicated with black arrow; the respective depth of the summer halocline, formed by the seasonal ice melt, is indicated for the salinity profiles. The salinities 33.1 and 34.2 indicate the mean salinities of the upper and lower haloclines, respectively.

OSD
9, 2621–2677, 2012

Time and space variability of freshwater content

M. Korhonen et al.

Title Page
Abstract | Introduction
Conclusions | References
Tables | Figures
◀| |▶
◀ ▶
Back | Close
Full Screen / Esc
Printer-friendly Version
Interactive Discussion

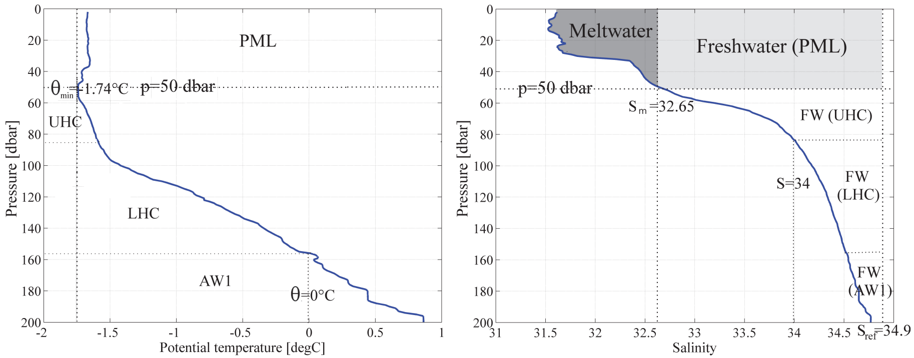

Fig. 4. The temperature and salinity profiles illustrating the integrated (Eq. 1) freshwater content in separate water masses. The meltwater content (dark grey) is distinguished from the freshwater content (light grey) in the Polar Mixed Layer (PML) by the salinity S_m at the depth of temperature minimum T_{min}.

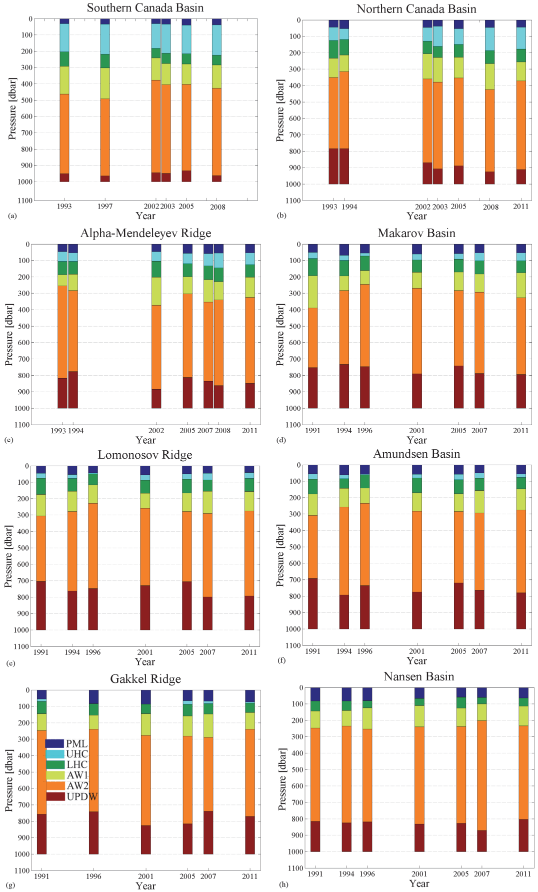

Fig. 5. Thickness of separate layers: Polar Mixed Layer (blue), upper halocline (cyan), lower halocline (green), upper Atlantic Water (yellow), lower Atlantic Water (orange), upper Polar Deep Water (red) in the different sub-areas in the Arctic Ocean. The thickness corresponds to volume in a water column with cross-section of 1 m^2 in the different areas.

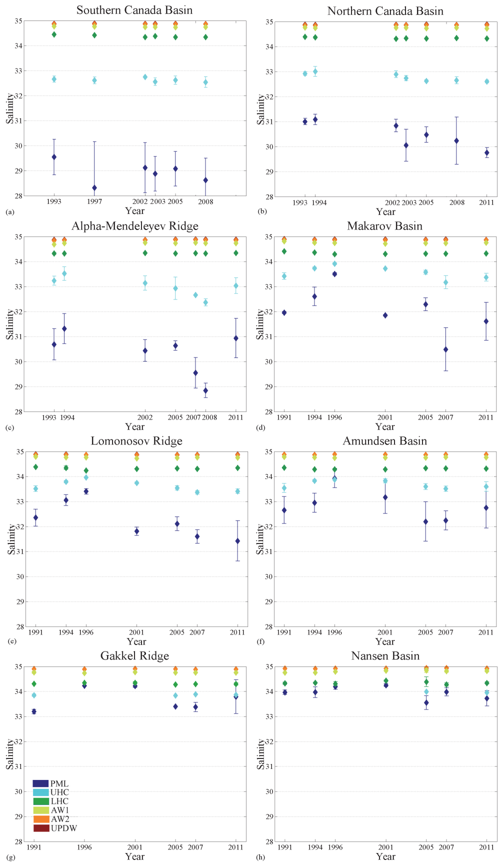

Fig. 6. The average salinity in the Polar Mixed Layer (blue), upper halocline (cyan), lower halocline (green), upper Atlantic Water (yellow), lower Atlantic Water (orange), upper Polar Deep Water (red) in the different sub-areas in the Arctic Ocean. Also the standard deviation within each basin is shown.

OSD
9, 2621–2677, 2012

Title Page
Abstract Introduction
Conclusions References
Tables Figures
◀| |▶
◀ ▶
Back Close
Full Screen / Esc
Printer-friendly Version
Interactive Discussion

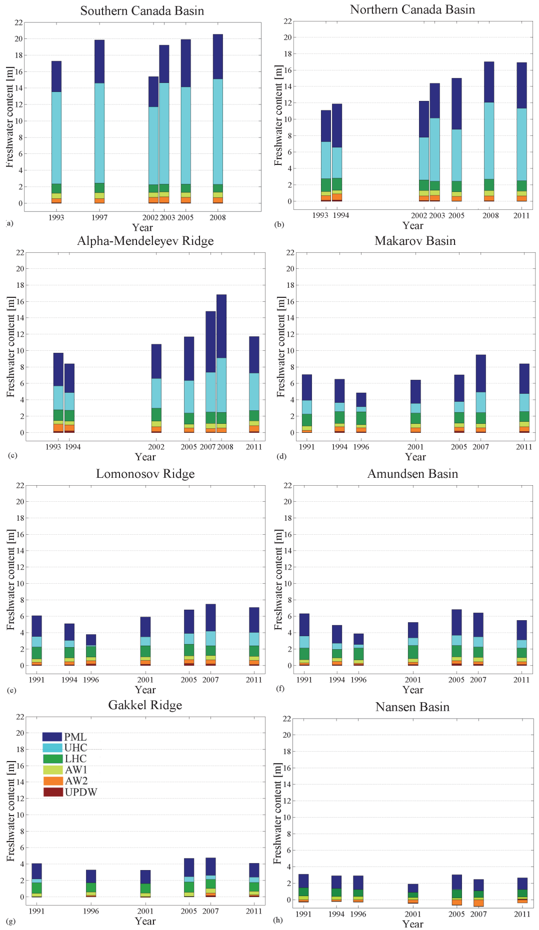

Fig. 7. The freshwater content in the Polar Mixed Layer (blue), upper halocline (cyan), lower halocline (green), upper Atlantic Water (yellow), lower Atlantic Water (orange), upper Polar Deep Water (red) in the different sub-areas in the Arctic Ocean.

OSD
9, 2621–2677, 2012

Time and space variability of freshwater content

M. Korhonen et al.

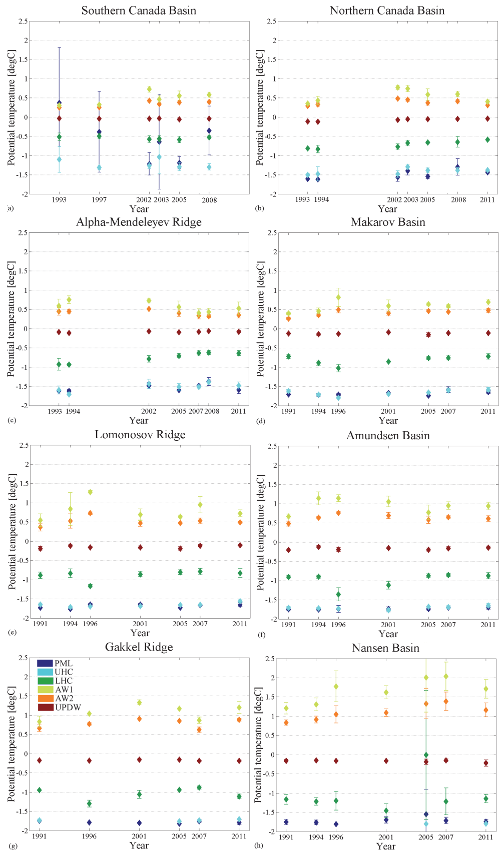

Fig. 8. The average potential temperature in the Polar Mixed Layer (blue), upper halocline (cyan), lower halocline (green), upper Atlantic Water (yellow), lower Atlantic Water (orange), upper Polar Deep Water (red) in the different sub-areas in the Arctic Ocean. Also the standard deviation within each basin is shown.

OSD
9, 2621–2677, 2012

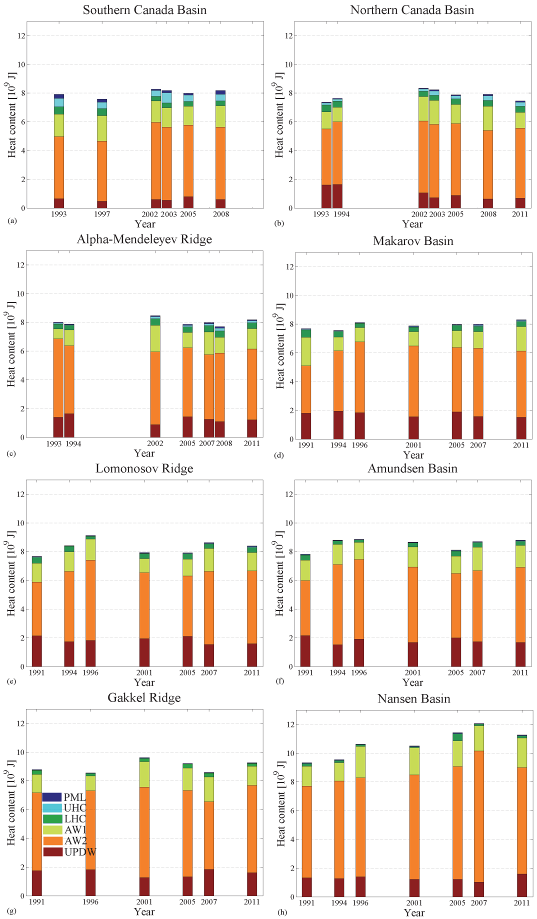

Fig. 9. The heat content in the Polar Mixed Layer (blue), upper halocline (cyan), lower halocline (green), upper Atlantic Water (yellow), lower Atlantic Water (orange), upper Polar Deep Water (red) in the different sub-areas in the Arctic Ocean.

OSD
9, 2621–2677, 2012

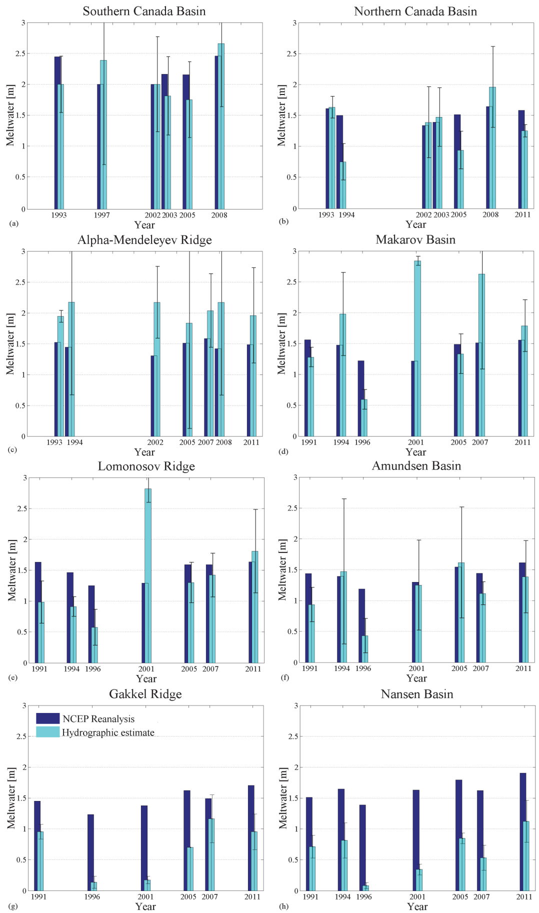

Fig. 10. The meltwater content estimated from the hydrographic data (cyan) compared to the estimated potential ice melt induced by the atmospheric surface fluxes (blue) in the different sub-areas in the Arctic Ocean. The standard deviation for the hydrographic estimate is shown.

OSD
9, 2621–2677, 2012

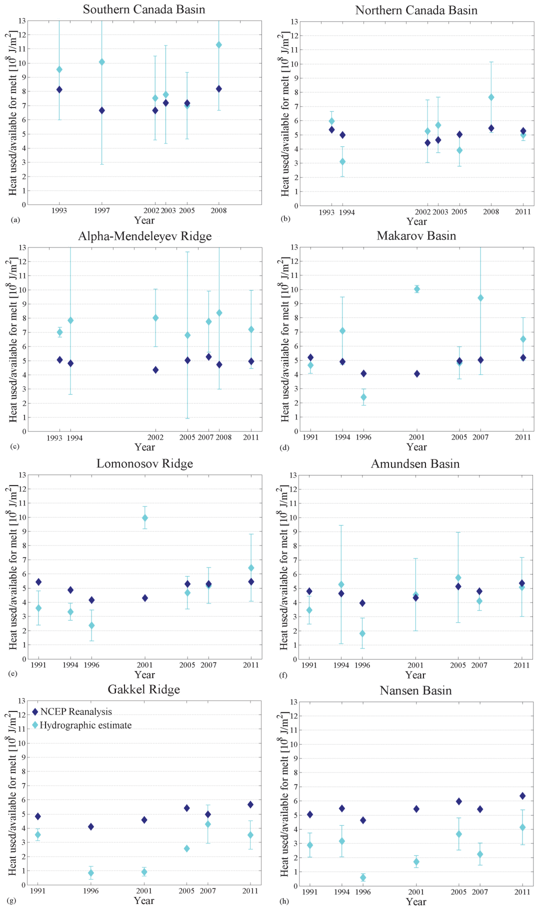

Fig. 11. The sum of heat needed to account for the estimated meltwater content and the heat stored in the Polar Mixed Layer (cyan) compared to the cumulative heat input based on the NCEP surface fluxes (blue) in the different sub-areas in the Arctic Ocean. The standard deviations for both are also shown.

OSD
9, 2621–2677, 2012

Time and space variability of freshwater content

M. Korhonen et al.

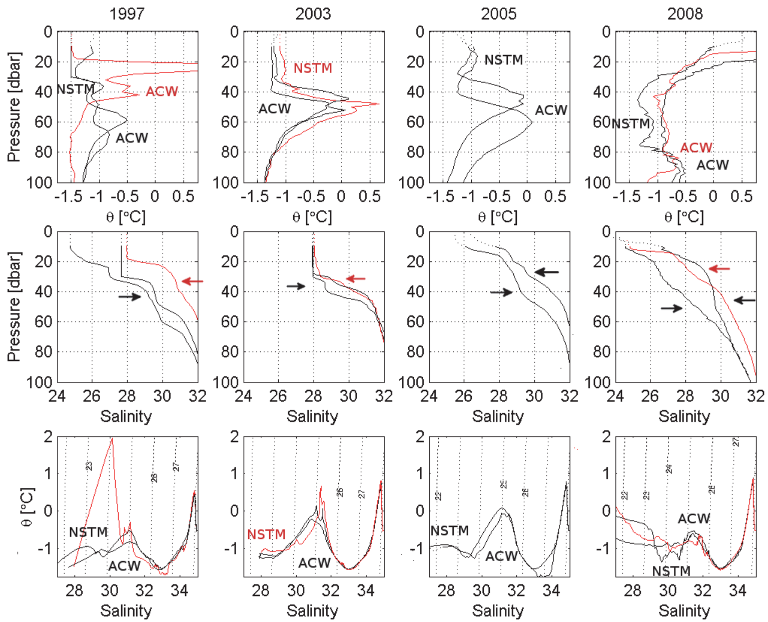

Fig. 12. Upper panel: Temperature profiles from the Southern Canada Basin representing the development of the near surface temperature maximum (NSTM) and the Alaskan Coastal Water (ACW). The casts are located in the Central Beaufort Sea (black) and east of the Chukchi Plateau at ~75° N (red). In 1997 the NSTM could have been merged with the pool of warm water, possibly deriving from the continental shelf. Middle panel: arrows indicate the depth of the Polar Mixed Layer and thus also the reference salinity for computing meltwater content, usually 29...30. The difficulties in defining the temperature minimum and the corresponding summer halocline are evident particularly in 2008. Also the extrapolation above 10 dbar (dotted line) yields the largest error in 2008. In 1997 two summer haloclines appear to be present, the lowest is chosen on the basis of the salinity, assumed to be near 30 at the base of the Polar Mixed Layer in the Canada Basin. Lower panel: the definition and characteristics of different water masses is best seen in θS-diagrams.

OSD
9, 2621–2677, 2012